94. Semileptonic B-Hadron Decays, Determination of V_{cb}, V_{ub}

Updated October 2017 by R. Kowalewski (Univ. of Victoria, Canada)
and T. Mannel (Univ. of Siegen, Germany)

94.1. Introduction

Precision determinations of $|V_{ub}|$ and $|V_{cb}|$ are central to testing the CKM sector of the Standard Model, and complement the measurements of CP asymmetries in B decays. The length of the side of the unitarity triangle opposite the well-measured angle β is proportional to the ratio $|V_{ub}|/|V_{cb}|$; its precise determination is a high priority of the heavy-flavor physics program.

The semileptonic transitions $b \to c\ell\bar{\nu}_\ell$ and $b \to u\ell\bar{\nu}_\ell$ (where ℓ refers to an electron or muon) each provide two avenues for determining these CKM matrix elements, namely through inclusive and exclusive final states. Recent measurements and calculations are reflected in the values quoted in this article, which is an update of the previous review [1]. The leptonic decay $B^- \to \tau\bar{\nu}$ can also be used to extract $|V_{ub}|$; we do not use this information at present since none of the experimental measurements has reached a competitive level of precision.

The theory underlying the determination of $|V_{qb}|$ is mature, in particular for $|V_{cb}|$. Most of the theoretical approaches use the fact that the mass m_b of the b quark is large compared to the scale $\Lambda_{\rm QCD}$ that determines low-energy hadronic physics. The basis for precise calculations is a systematic expansion in powers of Λ/m_b, where $\Lambda \sim 500 - 700$ MeV is a hadronic scale of the order of $\Lambda_{\rm QCD}$, based on effective-field-theory methods described in a separate RPP mini-review [2]. The use of lattice QCD for calculations of non-perturbative quantities plays an essential role in many of the determinations discussed here; lattice methods are discussed in a separate RPP mini-review [3].

The measurements discussed in this review are of branching fractions or ratios of branching fractions. The determinations of $|V_{cb}|$ and $|V_{ub}|$ also require a measurement of the total decay widths of the corresponding b hadrons, which is the subject of a separate RPP mini-review [4]. The measurements of inclusive semileptonic decays relevant to this review come primarily from e^+e^- B factories operating at the $\Upsilon(4S)$ resonance, where $B\bar{B}$ pairs are produced nearly at rest in the center-of-mass frame. Measurements of exclusive semileptonic decays come from the e^+e^- B factories and from the LHCb experiment at CERN.

Semileptonic B meson decay amplitudes to electrons and muons are assumed to be largely free from any impact of non-Standard Model physics, since they are dominated by Standard-Model W boson exchange. The decays $\bar{B} \to D^{(*)}\tau\bar{\nu}_\tau$, however, provide sensitivity to possible non-universalities in the couplings to the third generation leptons that are present at tree level in models involving new charged mediators. For example, a charged Higgs boson, present in many models of new physics, couples to the mass of the lepton and breaks lepton universality. If the enhanced decay rates seen in recent measurements of these decay modes turn out to be robust, they are an indication of new physics.

Many of the numerical results quoted in this review have been provided by the Heavy Flavor Averaging Group (HFLAV) [5].

94.2. Determination of $|V_{cb}|$

Summary: The determination of $|V_{cb}|$ from inclusive decays has a relative uncertainty of about 2%; the limitations arise mainly from our ignorance of higher-order perturbative and non-perturbative corrections. Exclusive $\bar{B} \to D^* \ell \bar{\nu}_\ell$ decays provide a determination of $|V_{cb}|$ with a relative precision of about 2%, with comparable contributions from theory and experiment; the value determined from $\bar{B} \to D \ell \bar{\nu}_\ell$ decays is consistent and has an uncertainty of 3%. However, as discussed below, recent work has raised questions about these determinations. We choose to quote a less constraining value from exclusive decays.

The values obtained from the inclusive and exclusive determinations discussed below are:

$$|V_{cb}| = (42.2 \pm 0.8) \times 10^{-3} \quad \text{(inclusive)} \tag{94.1}$$

$$|V_{cb}| = (41.9 \pm 2.0) \times 10^{-3} \quad \text{(exclusive).} \tag{94.2}$$

Assuming these determinations share a common 1% systematic uncertainty, their average is

$$|V_{cb}| = (42.2 \pm 0.8) \times 10^{-3} \quad \text{(average).} \tag{94.3}$$

94.2.1. $|V_{cb}|$ *from exclusive decays* :

Exclusive determinations of $|V_{cb}|$ make use of semileptonic B decays into the ground state charmed mesons D and D^* and are based on the distribution of the variable $w \equiv v \cdot v'$, where v and v' are the four velocities of the initial and final-state hadrons. In the rest frame of the decay this variable corresponds to the Lorentz factor of the final state $D^{(*)}$ meson. Heavy Quark Symmetry (HQS) [6,7] predicts these decay rates in the infinite mass limit in terms of a single form factor, which is normalized at $w = 1$, the point of maximum momentum transfer to the leptons. Measured decay rates and calculations of the form factors are used to determine $|V_{cb}|$.

A precise determination requires corrections to the HQS prediction for the normalization as well as some information on the shape of the form factors near the point $w = 1$. These calculations utilize Heavy Quark Effective Theory, which is discussed in a separate RPP mini-review [2]. Form factors that are normalized due to HQS are protected against linear corrections [8], and thus the leading corrections are of order $\Lambda^2_{\rm QCD}/m_c^2$. For the form factors that vanish in the infinite mass limit the corrections are in general linear in $\Lambda_{\rm QCD}/m_c$. In addition to these corrections, there are perturbatively calculable radiative corrections from hard gluons and photons, which will be discussed in the relevant sections.

94.2.2. $\bar{B} \to D^* \ell \bar{\nu}_\ell$:

The decay rate for $\bar{B} \to D^* \ell \bar{\nu}_\ell$ is given by

$$\frac{d\Gamma}{dw}(\bar{B} \to D^* \ell \bar{\nu}_\ell) = \frac{G_F^2 m_B^5}{48\pi^3} |V_{cb}|^2 (w^2-1)^{1/2} P(w) (\eta_{\rm ew} \mathcal{F}(w))^2, \tag{94.4}$$

where $P(w)$ is a phase space factor,

$$P(w) = r^3 (1-r)^2 (w+1)^2 \left(1 + \frac{4w}{w+1} \frac{1-2rw+r^2}{(1-r)^2}\right).$$

with $r = m_{D^*}/m_B$. The form factor $\mathcal{F}(w)$, which at $w = 1$ is unity by HQS in the infinite-mass limit, is dominated by the axial vector form factor h_{A_1} as $w \to 1$. For the definitions of the vector and axial vector form factors as a function of w, see Eq. (2.84) of the first paper of Ref. 9. The factor $\eta_{\rm ew} = 1.0066 \pm 0.0050$ accounts for the leading electroweak corrections to the four-fermion operator mediating the semileptonic decay [10], and includes an estimated uncertainty for missing long-distance QED radiative corrections [11].

The determination of V_{cb} involves an extrapolation to the zero-recoil point, for which a parametrization of $\mathcal{F}(w)$ is needed. Convenient parametrizations make use of analyticity and unitarity constraints on the the form factors and are expressed in terms of the variable

$$z = (\sqrt{w+1} - \sqrt{2})/(\sqrt{w+1} + \sqrt{2})\,, \tag{94.5}$$

originating from a conformal transformation. In terms of this variable the form factors (generically denoted as F) may be written as [13]

$$F(z) = \frac{1}{P_F(z)\phi_F(z)} \sum_{n=0}^{\infty} a_n z^n \tag{94.6}$$

where the sum $\sum |a_n|^2$ is bounded. Furthermore, the function $P(z)$ takes into account the resonances in the $(\bar{c}b)$ system below the $\bar{D}B$ threshold, and the weighting functions $\phi_F(z)$ are derived from the unitarity constraint on the corresponding form factor. The values of z relevant to the decay are $0 \le z \le 0.06$, hence the series in z converges rapidly and only very few terms are needed. Eq. (94.6) will be referred to as the "BGL" expansion.

A frequently used parametrization proposed in Ref. 14,

$$F(w) = F(1) - \rho^2(w-1) + c(w-1)^2 + \cdots\,,$$

has the slope ρ of the form factor as the only parameter. This "CLN" parameterization imposes a relation between the curvature c and the slope ρ based on the heavy quark limit. However, this seems to be too constraining given current experimental precision. More recent analyses [15,16] take this into account and include additional parameters using the BGL expansion. Very recently it has been pointed out these BGL fits are in tension with recent lattice data and would indicate large violations of heavy-quark symmetry [32].

The theoretical analysis of $F(1)$ includes the QCD short-distance radiative correction [17] to the form factor as well as the non-perturbative $1/m^2$ corrections, which can be calculated on the lattice (see below).

Precise lattice determinations of the $B \to D^{(*)}$ form factors use heavy-quark symmetries, so all uncertainties scale with the deviation of the form factor from unity. The state-of-the-art calculations are "unquenched", i.e. calculations with realistic sea quarks using $2+1$ flavors. The relevant calculations for the form factor $\mathcal{F}(\omega)$ in Ref. 11 quote a total uncertainty at the (1-2)% level. The main contributions to this uncertainty are from the chiral extrapolation from the light quark masses used in the numerical

lattice computation to realistic up and down quark masses, and from discretization errors. These sources of uncertainty will be reduced with larger lattice sizes and smaller lattice spacings. Including effects from finite quark masses to calculate the deviation of $\mathcal{F}(1)$ from unity, the current lattice prediction [11] is

$$\mathcal{F}(1) = 0.906 \pm 0.013, \tag{94.7}$$

We note that very recently an independent lattice result has been shown at a conference, indicating a lower value for $\mathcal{F}(1)$ [12].

Non-lattice estimates based on sum rules for the form factor tend to yield lower values for $\mathcal{F}(1)$ [18,19,20]. Omitting the contributions from excited states, the sum rules indicate that $\mathcal{F}(1) < 0.93$. Including an estimate for the contribution of the excited states yields $\mathcal{F}(1) = 0.86 \pm 0.01 \pm 0.02$ [20,21] where the second uncertainty accounts for the excited states.

Many experiments [22–31] have measured the differential decay rate as a function of w, employing a variety of methods: using either B^+ or B^0 decays, with or without B-tagging, and with or without explicit reconstruction of the transition pion from $D^* \to D$ decays. These measurements are input to a four-dimensional fit [5] for $\eta_{\rm ew}\mathcal{F}(1)|V_{cb}|$, $\rho^2_{A_1}$ and the form-factor ratios $R_1 \propto A_2/A_1$ and $R_2 \propto V/A_1$. The fit gives $\eta_{\rm ew}\mathcal{F}(1)\,|V_{cb}| = (35.61 \pm 0.43) \times 10^{-3}$ (LQCD, CLN) with a p-value of 0.14. The leading sources of uncertainty on $\eta_{\rm ew}\mathcal{F}(1)\,|V_{cb}|$ are due to detection efficiencies and $D^{(*)}$ decay branching fractions. Note that the $\bar{B} \to D^*\ell\bar{\nu}_\ell$ form factor in the fit is parameterized using the CLN form, which has the drawbacks discussed previously.

A safer approach is to use the more general BGL form-factor parameterization. At present, only one measurement [31] has published the unfolded fully-differential decay rate and associated covariance matrix. Using this input, two analyses [15,16] have recently shown $\sim 10\%$ shifts in $\eta_{\rm ew}\mathcal{F}(1)|V_{cb}|$ when switching from the CLN to the BGL form, well beyond the quoted experimental precision. These analyses are consistent with each other and give [15] $\eta_{\rm ew}\mathcal{F}(1)\,|V_{cb}| = (38.2\ ^{+1.7}_{-1.6}) \times 10^{-3}$. Along with the lattice value given above for $\mathcal{F}(1)$ this yields

$$|V_{cb}| = (41.9\ ^{+2.0}_{-1.9}) \times 10^{-3}\ (\bar{B} \to D^*\ell\bar{\nu}_\ell,\ \text{LQCD, BGL}). \tag{94.8}$$

It has been pointed out [32] that fits to these data with the BGL parameterization are in tension with HQET and lattice predictions for form-factor ratios. More work is needed to clarify these issues.

94.2.3. $\bar{B} \to D\ell\bar{\nu}_\ell$:

The differential rate for $\bar{B} \to D\ell\bar{\nu}_\ell$ is given by

$$\frac{d\Gamma}{dw}(\bar{B} \to D\ell\bar{\nu}_\ell) =$$

$$\frac{G_F^2}{48\pi^3}|V_{cb}|^2(m_B + m_D)^2 m_D^3 (w^2-1)^{3/2}(\eta_{\rm ew}\mathcal{G}(w))^2. \tag{94.9}$$

The form factor is

$$\mathcal{G}(w) = h_+(w) - \frac{m_B - m_D}{m_B + m_D} h_-(w), \tag{94.10}$$

where h_+ is normalized to unity due to HQS and h_- vanishes in the infinite-mass limit. Thus

$$\mathcal{G}(1) = 1 + \mathcal{O}\left(\frac{m_B - m_D}{m_B + m_D}\frac{\Lambda_{\rm QCD}}{m_c}\right) \tag{94.11}$$

and the corrections to the HQET predictions are parametrically larger than was the case for $\bar{B} \to D^* \ell \bar{\nu}_\ell$.

Lattice calculations including effects beyond the heavy mass limit have become available, and hence the fact that deviations from the HQET predictions are parametrically larger than for $\bar{B} \to D^* \ell \bar{\nu}_\ell$ is irrelevant. These unquenched calculations provide information over a range of z values (see Eq. (94.5)) and can be used in a simultaneous fit, along with the differential branching fraction, in a form-factor expansion in z [13,33]. This is important, since the experimental precision near $w = 1$ is poor given the low decay rate in this region.

From lattice simulations one obtains the form factor normalization at zero recoil; the currently most precise value [34] is

$$\mathcal{G}(1) = 1.054 \pm 0.004 \pm 0.008 \ . \tag{94.12}$$

The most precise measurements of $\bar{B} \to D \ell \bar{\nu}_\ell$ [29,35,36] dominate the average [5] value, $\eta_{\rm ew}\mathcal{G}(1)|V_{cb}| = (41.57 \pm 1.00) \times 10^{-3}$. Note that this average corresponds to measurements that fit to the CLN form factor parameterization; the same concerns expressed above for $\bar{B} \to D^* \ell \bar{\nu}_\ell$ apply here. Using the value from Eq. (94.12) for $\mathcal{G}(1)$ and accounting for the electroweak correction as above gives

$$|V_{cb}| = (39.18 \pm 0.94 \pm 0.36) \times 10^{-3} \ \ (\bar{B} \to D \ell \bar{\nu}_\ell, \ \text{LQCD, CLN}), \tag{94.13}$$

where the first uncertainty is from experiment, the second from lattice QCD and the electroweak and Coulomb corrections.

The $|V_{cb}|$ averages from $\bar{B} \to D^* \ell \bar{\nu}_\ell$ and $\bar{B} \to D \ell \bar{\nu}_\ell$ decays using the CLN form are consistent; however, these determinations need to be redone using the more general BGL parameterization. We choose to quote the result in Eq. (94.8):

$$|V_{cb}| = (41.9\ ^{+2.0}_{-1.9}) \times 10^{-3} \quad \text{(exclusive)}. \tag{94.14}$$

94.2.4. ***$|V_{cb}|$ from inclusive decays*** :

Measurements of the total semileptonic branching decay rate, along with moments of the lepton energy and hadronic invariant mass spectra in inclusive semileptonic $b \to c$ transitions, can be used to determine $|V_{cb}|$. The total semileptonic decay rate can be calculated quite reliably in terms of non-perturbative parameters that can be extracted from the information contained in the moments.

94.2.5. ***Inclusive semileptonic rate*** :

The theoretical foundation for the calculation of the total semileptonic rate is the Operator Product Expansion (OPE) which yields the Heavy Quark Expansion (HQE) [37,38]. Details can be found in the RPP mini-review on Effective Theories [2].

The OPE result for the total rate can be written schematically (details can be found, *e.g.*, in Ref. 39) as

$$\begin{aligned}\Gamma =& |V_{cb}|^2 \frac{G_F^2 m_b^5(\mu)}{192\pi^3}(1+A_{\rm ew})\times \\ & \left[z_0^{(0)}(r) + \frac{\alpha_s(\mu)}{\pi} z_0^{(1)}(r) + \left(\frac{\alpha_s(\mu)}{\pi}\right)^2 z_0^{(2)}(r) + \cdots \right. \\ & + \frac{\mu_\pi^2}{m_b^2}\left(z_2^{(0)}(r) + \frac{\alpha_s(\mu)}{\pi} z_2^{(1)}(r) + \cdots \right) \\ & + \frac{\mu_G^2}{m_b^2}\left(y_2^{(0)}(r) + \frac{\alpha_s(\mu)}{\pi} y_2^{(1)}(r) + \cdots \right) \\ & + \frac{\rho_{\rm D}^3}{m_b^3}\left(z_3^{(0)}(r) + \frac{\alpha_s(\mu)}{\pi} z_3^{(1)}(r) + \cdots \right) \\ & \left. + \frac{\rho_{\rm LS}^3}{m_b^3}\left(y_3^{(0)}(r) + \frac{\alpha_s(\mu)}{\pi} y_3^{(1)}(r) + \cdots \right) + ... \right] \end{aligned} \tag{94.15}$$

where $\eta_{\rm ew} = 1 + A_{\rm ew}$ denotes the electroweak corrections, r is the ratio m_c/m_b and the y_i and z_i are functions that appear in the perturbative expansion at different orders of the heavy mass expansion. The parameters μ_π, μ_G, ρ_D and ρ_{LS} constitute the non-perturbative input into the heavy quark expansion; they correspond to certain matrix elements to be discussed below. In the same way the HQE can be set up for the moments of distributions of charged-lepton energy, hadronic invariant mass and hadronic energy, e.g.

$$\langle E_e^n \rangle_{E_e > E_{\rm cut}} = \int_{E_{\rm cut}}^{E_{\rm max}} \frac{d\Gamma}{dE_e} E_e^n dE_e \Bigg/ \int_{E_{\rm cut}}^{E_{\rm max}} \frac{d\Gamma}{dE_e} dE_e \ .$$

The coefficients of the HQE are known up to order $1/m_b^5$ at tree level [40–43]. The leading term is the parton model, and is known completely to order α_s and α_s^2 [44–46]; the terms of order $\alpha_s^{n+1}\beta_0^n$ (where β_0 is the first coefficient of the QCD β function, $\beta_0 = (33 - 2n_f)/3$) have been included by the usual BLM procedure [39,47,48].

Corrections of order $\alpha_s\mu_\pi^2/m_b^2$ have been computed in Refs. 49 and 50, while the $\alpha_s\mu_G^2/m_b^2$ terms have been calculated in Refs. 51 and 52.

Starting at order $1/m_b^3$ contributions with an infrared sensitivity to the charm mass, m_c, appear [42,53,54]. At order $1/m_b^3$ this "intrinsic charm" contribution manifests as a $\log(m_c)$ in the coefficient of the Darwin term ρ_D^3. At higher orders, terms such as $1/m_b^3 \times 1/m_c^2$ and $\alpha_s(m_c)1/m_b^3 \times 1/m_c$ appear, which are comparable in size to the contributions of order $1/m_b^4$

The HQE parameters are given in terms of forward matrix elements; the parameters entering the expansion for orders up to $1/m_b^3$ are ($D_\perp^\mu = (g_{\mu\nu} - v_\mu v_\nu)D^\nu$)

$$\begin{aligned}
\overline{\Lambda} &= M_B - m_b\,, \\
\mu_\pi^2 &= -\langle B|\bar{b}(iD_\perp)^2 b|B\rangle\,, \\
\mu_G^2 &= \langle B|\bar{b}(iD_\perp^\mu)(iD_\perp^\nu)\sigma_{\mu\nu} b|B\rangle\,, \\
\rho_{\rm D}^3 &= \langle B|\bar{b}(iD_{\perp\mu})(ivD)(iD_\perp^\nu) b|B\rangle\,, \\
\rho_{\rm LS}^3 &= \langle B|\bar{b}(iD_\perp^\mu)(ivD)(iD_\perp^\nu)\sigma_{\mu\nu} b|B\rangle. \qquad (94.16)
\end{aligned}$$

These parameters still depend on the heavy quark mass. Sometimes the infinite mass limits of these parameters $\overline{\Lambda} \to \overline{\Lambda}_{\rm HQET}$, $\mu_\pi^2 \to -\lambda_1$, $\mu_G^2 \to 3\lambda_2$, $\rho_D^3 \to \rho_1$ and $\rho_{LS}^3 \to 3\rho_2$, are used instead. The hadronic parameters of the orders $1/m_b^4$ and $1/m_b^5$ have been defined and estimated in Ref. 43. The five hadronic parameters s_i of the order $1/m_b^4$ can be found in Ref. 41. These terms have not yet been included in the fits.

The rates and the spectra depend strongly on m_b (or equivalently on $\overline{\Lambda}$). This makes the discussion of renormalization issues mandatory, since the size of QCD corrections is strongly correlated with the definitions used for the quark masses. For example, it is well known (see eg. [55]) that using the pole mass definition for heavy quark masses leads to a perturbative series for the decay rates that does not converge very well, making a precision determination of $|V_{cb}|$ in such a scheme impossible.

This motivates the use of "short-distance" mass definitions, such as the kinetic scheme [18] or the 1S scheme [56]. Both schemes have been applied to semileptonic $b \to c$ transitions and yield comparable results and uncertainties. The 1S scheme eliminates the b quark pole mass by relating it to the perturbative expression for the mass of the 1S state of the Υ system. The physical mass of the $\Upsilon(1S)$ contains non-perturbative contributions, which have been estimated in Ref. 57. These non-perturbative contributions are small; nevertheless, the best determination of the b quark mass in the 1S scheme is obtained from sum rules for $e^+e^- \to b\bar{b}$ [58]. Alternatively one may use a short-distance mass definition such as the $\overline{\rm MS}$ mass, $m_b^{\overline{\rm MS}}(m_b)$. However, it has been argued that the scale m_b is unnaturally high for B decays, while for smaller scales $\mu \sim 1\,{\rm GeV}$ $m_b^{\overline{\rm MS}}(\mu)$ is under poor control. For this reason the so-called "kinetic mass" $m_b^{\rm kin}(\mu)$, has been proposed. It is the mass entering the non-relativistic expression for the kinetic energy of a heavy quark, and is defined using heavy-quark sum rules [18].

94.2.6. *Determination of HQE Parameters and* $|V_{cb}|$:

Several experiments have measured moments in $\bar{B} \to X_c \ell \bar{\nu}_\ell$ decays [59–67] as a function of the minimum lepton momentum. The measurements of the moments of the electron energy spectrum (0^{th}-3^{rd}) and of the squared hadronic mass spectrum (0^{th}-2^{nd}) have statistical uncertainties that are roughly equal to their systematic uncertainties. The sets of moments measured within each experiment have strong correlations; their use in a global fit requires fully specified statistical and systematic covariance matrices. Measurements of photon energy moments (0^{th}-2^{nd}) in $B \to X_s\gamma$ decays [68–72] as a function of the minimum accepted photon energy are also used in some fits; the dominant uncertainties on these measurements are statistical.

Global fits [67,69,73–78] to the full set of moments have been performed in the 1S and kinetic schemes. The semileptonic moments alone determine a linear combination of m_b and m_c very accurately but leave the orthogonal combination poorly determined [79]; additional input is required to allow a precise determination of m_b. This additional information can come from the radiative $B \to X_s\gamma$ moments (with the caveat that the OPE for $b \to s\gamma$ breaks down beyond leading order in Λ_{QCD}/m_b), which provide complementary information on m_b and μ_π^2, or from precise determinations of the charm quark mass [80,81]. The values obtained in the kinetic scheme fits [75,77,78] with these two constraints are consistent. Based on the charm quark mass constraint $m_c^{\overline{\text{MS}}}(3\,\text{GeV}) = 0.986 \pm 0.013\,\text{GeV}$ [82], a fit in the kinetic scheme [5] obtains

$$|V_{cb}| = (42.19 \pm 0.78) \times 10^{-3} \tag{94.17}$$

$$m_b^{\text{kin}} = 4.554 \pm 0.018\,\text{GeV} \tag{94.18}$$

$$\mu_\pi^2(\text{kin}) = 0.464 \pm 0.076\,\text{GeV}^2, \tag{94.19}$$

where the errors include experimental and theoretical uncertainties.

Theoretical uncertainties from higher orders in $1/m$ as well as in α_s are estimated and included in performing the fits. Similar values for the parameters are obtained with a variety of assumptions about the theoretical uncertainties and their correlations. The χ^2/dof is substantially below unity in all fits, which could suggest that the theoretical uncertainties may be overestimated. However, while one could obtain a satisfactory fit with smaller uncertainties, this would result in unrealistically small uncertainties on the extracted HQE parameters, which are used as input to other calculations (e.g. the determination of $|V_{ub}|$). In any case, the low χ^2 shows no evidence for duality violations at a significant level. The mass in the $\overline{\text{MS}}$ scheme corresponding to Eq. (94.18) is $m_b^{\overline{\text{MS}}} = 4.19 \pm 0.04\,\text{GeV}$, where the uncertainty includes a contribution from the translation between mass schemes; this can be compared with a value obtained using relativistic sum rules [82], $m_b^{\overline{\text{MS}}} = 4.163 \pm 0.016\,\text{GeV}$, which provides a non-trivial cross-check.

A fit to the measured moments in the 1S scheme [76,5] gives

$$|V_{cb}| = (41.98 \pm 0.45) \times 10^{-3} \tag{94.20}$$

$$m_b^{\text{1S}} = 4.691 \pm 0.037\,\text{GeV} \tag{94.21}$$

$$\lambda_1(\text{1S}) = -0.362 \pm 0.067\,\text{GeV}^2, \tag{94.22}$$

This fit uses semileptonic and radiative moments and constrains the chromomagnetic operator using the B^*-B and D^*-D mass differences, but does not include the constraint on m_c nor the full NNLO corrections.

The fits in the two renormalization schemes give consistent results for $|V_{cb}|$ and, after translation to a common renormalization scheme, for m_b and μ_π^2. We take the fit in the kinetic scheme [78], which includes higher-order corrections and results in a more conservative uncertainty, as the inclusive determination of $|V_{cb}|$:

$$|V_{cb}| = (42.2 \pm 0.8) \times 10^{-3} \text{ (inclusive)}. \tag{94.23}$$

The precision of the global fit results can be further improved by calculating higher-order perturbative corrections to the coefficients of the HQE parameters, in particular the still-missing $\alpha_s \mu_G^2$ corrections, which are presently only known for $B \to X_s\gamma$ [83]. The inclusion of still-higher-order moments, if they can be measured with the required precision, may improve the sensitivity of the fits to higher-order terms in the HQE.

94.3. Determination of $|V_{ub}|$

Summary: The best determinations of $|V_{ub}|$ are from $\bar{B} \to \pi \ell \bar{\nu}_\ell$ decays, where combined fits to theory and experimental data as a function of q^2 provide a precision below 5%; the uncertainties from experiment and theory are comparable in size. Determinations based on inclusive semileptonic decays are done based on different observables and using different calculational ansatzes. All determinations are consistent and provide a precision of about 6%, with comparable contributions to the uncertainty from experiment and theory.

The values obtained from inclusive and exclusive determinations are

$$|V_{ub}| = (4.49 \pm 0.15 \,{}^{+\,0.16}_{-\,0.17} \pm 0.17) \times 10^{-3} \quad \text{(inclusive)}, \tag{94.24}$$

$$|V_{ub}| = (3.70 \pm 0.10 \pm 0.12) \times 10^{-3} \quad \text{(exclusive)}, \tag{94.25}$$

where the last uncertainty on the inclusive result was added by the authors of this review and is discussed below. The two determinations are independent, and the dominant uncertainties are on multiplicative factors. To combine these values, the inclusive and exclusive values are weighted by their relative errors and the uncertainties are treated as normally distributed. The resulting average has $p(\chi^2) = 0.9\%$, so we scale the error by $\sqrt{\chi^2/1} = 2.6$ to find

$$|V_{ub}| = (3.94 \pm 0.36) \times 10^{-3} \quad \text{(average)}. \tag{94.26}$$

Given the poor consistency between the two determinations, this average should be treated with caution.

94.3.1. $|V_{ub}|$ *from inclusive decays* :

The theoretical description of inclusive $\bar{B} \to X_u \ell \bar{\nu}_\ell$ decays is based on the Heavy Quark Expansion, as for $\bar{B} \to X_c \ell \bar{\nu}_\ell$ decays, and leads to a predicted total decay rate with uncertainties below 5% [84,85]. Unfortunately, the total decay rate is hard to measure due to the large background from CKM-favored $\bar{B} \to X_c \ell \bar{\nu}_\ell$ transitions. Technically, the calculation of the partial decay rate in regions of phase space where $\bar{B} \to X_c \ell \bar{\nu}_\ell$ decays are suppressed requires the introduction of a non-perturbative distribution function, the "shape function" (SF) [86,87], whose form is unknown. The shape function becomes important when the light-cone momentum component $P_+ \equiv E_X - |P_X|$ is not large compared to Λ_{QCD}, as is the case near the endpoint of the $\bar{B} \to X_u \ell \bar{\nu}_\ell$ lepton spectrum. Partial rates for $\bar{B} \to X_u \ell \bar{\nu}_\ell$ are predicted and measured in a variety of kinematic regions that differ in their sensitivity to shape-function effects.

At leading order a single shape function appears, which is universal for all heavy-to-light transitions [86,87] and can be measured in $\bar{B} \to X_s \gamma$ decays. At subleading order in $1/m_b$, several shape functions appear [88]. Thus, prescriptions that relate directly the partial rates for $\bar{B} \to X_s \gamma$ and $\bar{B} \to X_u \ell \bar{\nu}_\ell$ decays [89–92] are limited to leading order in $1/m_b$.

Existing approaches have tended to use parameterizations of the leading SF that respect constraints on the normalization and on the first and second moments, which are given in terms of the HQE parameters $\overline{\Lambda} = M_B - m_b$ and μ_π^2, respectively. The relations between SF moments and HQE parameters are known to second order in α_s [93]. As a result, measurements of HQE parameters from global fits to $\bar{B} \to X_c \ell \bar{\nu}_\ell$ and $\bar{B} \to X_s \gamma$ moments can be used to constrain the SF moments, as well as to provide accurate values of m_b and other parameters for use in determining $|V_{ub}|$. Flexible parameterizations of the SF using orthogonal basis functions [94] or artificial neural networks [95] would allow global fits to inclusive B meson decay data that incorporate the known short-distance contributions and renormalization properties of the SF.

HFLAV performs fits on the basis of several approaches, with varying degrees of model dependence. We will consider here the approaches documented in Ref. 97 (BLNP), Ref. 98 (GGOU) and Ref. 99 (DGE).

The triple diffential rate in the variables

$$P_l = M_B - 2E_l, \quad P_- = E_X + |\vec{P}_X|, \quad P_+ = E_X - |\vec{P}_X| \tag{94.27}$$

is

$$\frac{d^3\Gamma}{dP_+\, dP_-\, dP_l} = \frac{G_F^2 |V_{ub}|^2}{16\pi^2}(M_B - P_+) \tag{94.28}$$

$$\Big\{(P_- - P_l)(M_B - P_- + P_l - P_+)\mathcal{F}_1$$

$$+(M_B - P_-)(P_- - P_+)\mathcal{F}_2 + (P_- - P_l)(P_l - P_+)\mathcal{F}_3\Big\}\,.$$

The "structure functions" $\mathcal{F}_i$ can be calculated using factorization theorems that have been proven to subleading order in the $1/m_b$ expansion [96].

The BLNP [97] calculation uses these factorization theorems to write the $\mathcal{F}_i$ in terms of perturbatively calculable hard coefficients H and jet functions J, which are convolved with the (soft) light-cone distribution functions S, the shape functions of the B meson. The calculation of $\mathcal{O}(\alpha_S^2)$ contributions [101,102] is not yet complete and is not included in the $|V_{ub}|$ determination given below.

The leading order term in the $1/m_b$ expansion of the $\mathcal{F}_i$ contains a single non-perturbative function and is calculated to subleading order in α_s, while at subleading order in the $1/m_b$ expansion there are several independent non-perturbative functions that have been calculated only at tree level in the α_s expansion.

A distinct approach (GGOU) [98] uses a hard, Wilsonian cut-off that matches the definition of the kinetic mass. The non-perturbative input is similar to what is used in BLNP, but the shape functions are defined differently. In particular, they are defined at finite m_b and depend on the light-cone component k_+ of the b quark momentum and on the momentum transfer q^2 to the leptons. These functions include subleading effects to all orders; as a result they are non-universal, with one shape function corresponding to each structure function in Eq. (94.28). Their k_+ moments can be computed in the OPE and related to observables and to the shape functions defined in Ref. 97.

Going to subleading order in α_s requires the definition of a renormalization scheme for the HQE parameters and for the SF. The relation between the moments of the SF and the forward matrix elements of local operators is plagued by ultraviolet problems and requires additional renormalization. A scheme for improving this behavior was suggested in Refs. 97 and 103, which introduce a definition of the quark mass (the so-called shape-function scheme) based on the first moment of the measured $\bar{B} \to X_s\gamma$ photon energy spectrum. Likewise, the HQE parameters can be defined from measured moments of spectra, corresponding to moments of the SF.

One can attempt to calculate the SF by using additional assumptions. One approach (DGE) is the so-called "dressed gluon exponentiation" [99], where the perturbative result is continued into the infrared regime using the renormalon structure obtained in the large β_0 limit, where β_0 has been defined following Eq. (94.15).

In order to reduce sensitivity to SF uncertainties, measurements that use a combination of cuts on the leptonic momentum transfer q^2 and the hadronic invariant mass m_X, as suggested in Ref. 100, have been made. In general, efforts to extend the experimental measurements of $\bar{B} \to X_u\ell\bar{\nu}_\ell$ into charm-dominated regions (in order to reduce SF uncertainties) lead to an increased experimental sensitivity to the modeling of $\bar{B} \to X_u\ell\bar{\nu}_\ell$ decays, resulting in measured partial rates with an undesirable level of model dependence. The measurements quoted below have used a variety of functional forms to parameterize the leading SF; a specific error budget for one determination is quoted in the next section. In no case is the parameterization uncertainty estimated to be more than a 2% on $|V_{ub}|$.

Weak Annihilation [104,105,98] (WA) can in principle contribute significantly in the high-q^2 region of $\bar{B} \to X_u\ell\bar{\nu}_\ell$ decays. Estimates based on semileptonic D_s decays [105,54,100] lead to a $\sim 2\%$ uncertainty on the total $\bar{B} \to X_u\ell\bar{\nu}_\ell$ rate from the $\Upsilon(4S)$. The q^2 spectrum of the WA contribution is not well known, but from the OPE it is expected to contribute predominantly at high q^2. More recent theoretical investigations

[54,106,107] and a direct search [108] indicate that WA is a small effect, but may become a significant source of uncertainty for $|V_{ub}|$ measurements that accept only a small fraction of the full $\bar{B} \to X_u \ell \bar{\nu}_\ell$ phase space.

94.3.2. *Measurements* :

We summarize the measurements used in the determination of $|V_{ub}|$ below. Given the improved precision and more rigorous theoretical interpretation of more recent measurements, determinations [109–112] done at LEP are not considered in this review.

Inclusive electron momentum measurements [113–115] reconstruct a single charged electron to determine a partial decay rate for $\bar{B} \to X_u \ell \bar{\nu}_\ell$ near the kinematic endpoint. This results in a selection efficiency of order 50% and only modest sensitivity to the modeling of detector response. The inclusive electron momentum spectrum from $B\bar{B}$ events, after subtraction of the $e^+e^- \to q\bar{q}$ continuum background, is fitted to a model $\bar{B} \to X_u \ell \bar{\nu}_\ell$ spectrum and several components ($D\ell\bar{\nu}_\ell$, $D^*\ell\bar{\nu}_\ell$, ...) of the $\bar{B} \to X_c \ell \bar{\nu}_\ell$ background; the dominant uncertainties are related to this subtraction and modelling. The decay rate can be cleanly extracted for $E_e > 2.3\,\mathrm{GeV}$, but this is deep in the SF region, where theoretical uncertainties are large. The resulting $|V_{ub}|$ values for various E_e cuts are given in Table 94.1; the measurements listed there do not include the most recent determination from the electron momentum spectrum,which is discussed below.

An untagged "neutrino reconstruction" measurement [116] from BABAR uses a combination [117] of a high-energy electron with a measurement of the missing momentum vector. This allows S/B$\sim$ 0.7 for $E_e > 2.0\,\mathrm{GeV}$ and a $\approx 5\%$ selection efficiency, but at the cost of a smaller accepted phase space for $\bar{B} \to X_u \ell \bar{\nu}_\ell$ decays and uncertainties associated with the determination of the missing momentum. The corresponding values for $|V_{ub}|$ are given in Table 94.1.

The large samples accumulated at the B factories allow studies in which one B meson is fully reconstructed and the recoiling B decays semileptonically [118–122]. The experiments can fully reconstruct a "tag" B candidate in about 0.5% (0.3%) of B^+B^- ($B^0\bar{B}^0$) events. An electron or muon with center-of-mass momentum above 1.0 GeV is required amongst the charged tracks not assigned to the tag B and the remaining particles are assigned to the X_u system. The full set of kinematic properties (E_ℓ, m_X, q^2, *etc.*) are available for studying the semileptonically decaying B, making possible selections that accept up to 90% of the full $\bar{B} \to X_u \ell \bar{\nu}_\ell$ rate; however, the sensitivity to $\bar{B} \to X_u \ell \bar{\nu}_\ell$ decays is still driven by the regions where $\bar{B} \to X_c \ell \bar{\nu}_\ell$ decays are suppressed. Despite requirements (e.g. on the square of the missing mass) aimed at rejecting events with additional missing particles, undetected or mis-measured particles from $\bar{B} \to X_c \ell \bar{\nu}_\ell$ decay (e.g., K_L^0 and additional neutrinos) remain an important source of uncertainty.

BABAR [118] and Belle [119,120] have measured partial rates with cuts on m_X, m_X and q^2, P_+ and E_ℓ using the recoil method. In each case the experimental systematics have significant contributions from the modeling of $\bar{B} \to X_u \ell \bar{\nu}_\ell$ and $\bar{B} \to X_c \ell \bar{\nu}_\ell$ decays and from the detector response to charged particles, photons and neutral hadrons. The corresponding $|V_{ub}|$ values are given in Table 94.1.

94.3.3. $|V_{ub}|$ *from inclusive partial rates* :

The measured partial rates and theoretical calculations from BLNP, GGOU and DGE described previously are used to determine $|V_{ub}|$ from all measured partial $\bar{B} \to X_u \ell \bar{\nu}_\ell$ rates [5]; selected values are given in Table 94.1. The correlations amongst the multiple BABAR recoil-based measurements [118] are fully accounted for in the average. The statistical correlations amongst the other measurements used in the average are tiny (due to small overlaps among signal events and large differences in S/B ratios) and have been ignored. Correlated systematic and theoretical errors are taken into account, both within an experiment and between experiments. As an illustration of the relative sizes of the uncertainties entering $|V_{ub}|$ we give the error breakdown for the GGOU average: statistical—2.0%; experimental—1.7%; $\bar{B} \to X_c \ell \bar{\nu}_\ell$ modeling—1.3%; $\bar{B} \to X_u \ell \bar{\nu}_\ell$ modeling—1.8%; HQE parameters (m_b) —1.4%; higher-order corrections—1.5%; q^2 modeling—1.2%; Weak Annihilation—$^{+0.0}_{-1.9}$%; SF parameterization—0.2%.

The averages quoted here are based on the following m_b values: $m_b^{SF} = 4.582 \pm 0.023 \pm 0.018$ GeV for BLNP, $m_b^{\rm kin} = 4.554 \pm 0.018$ GeV for GGOU, and $m_b^{\overline{MS}} = 4.188 \pm 0.043$ GeV for DGE. The $m_b^{\rm kin}$ value is determined in a global fit to moments in the kinetic scheme; this value is translated into m_b^{SF} and $m_b^{\overline{MS}}$ at fixed order in α_s. The second uncertainty quoted on m_b arises from the scheme translation.

Table 94.1: $|V_{ub}|$ (in units of 10^{-5}) from inclusive $\bar{B} \to X_u \ell \bar{\nu}_\ell$ measurements. The first uncertainty on $|V_{ub}|$ is experimental, while the second includes both theoretical and HQE parameter uncertainties. The values are listed in order of increasing kinematic acceptance f_u (0.19 to 0.90); those below the horizontal bar are based on recoil methods.

Ref.	cut (GeV)	BLNP	GGOU	DGE
[113]	$E_e > 2.1$	$422 \pm 49 \,^{+\,29}_{-\,34}$	$423 \pm 49 \,^{+\,22}_{-\,31}$	$386 \pm 45 \,^{+\,25}_{-\,27}$
[116]	$E_e - q^2$	$471 \pm 32 \,^{+\,33}_{-\,38}$	not available	$435 \pm 29 \,^{+\,28}_{-\,30}$
[115]	$E_e > 2.0$	$452 \pm 26 \,^{+\,26}_{-\,30}$	$452 \pm 26 \,^{+\,17}_{-\,24}$	$430 \pm 24 \,^{+\,23}_{-\,25}$
[114]	$E_e > 1.9$	$493 \pm 46 \,^{+\,26}_{-\,29}$	$495 \pm 46 \,^{+\,16}_{-\,21}$	$482 \pm 45 \,^{+\,23}_{-\,23}$
[118]	$\substack{q^2>8 \\ m_X<1.7}$	$432 \pm 23 \,^{+\,26}_{-\,28}$	$433 \pm 23 \,^{+\,24}_{-\,27}$	$424 \pm 22 \,^{+\,18}_{-\,21}$
[118]	$P_+ < 0.66$	$409 \pm 25 \,^{+\,25}_{-\,25}$	$425 \pm 26 \,^{+\,26}_{-\,27}$	$417 \pm 25 \,^{+\,28}_{-\,37}$
[118]	$m_X < 1.7$	$403 \pm 22 \,^{+\,22}_{-\,22}$	$410 \pm 23 \,^{+\,16}_{-\,17}$	$422 \pm 23 \,^{+\,21}_{-\,27}$
[118]	$E_\ell > 1$	$433 \pm 24 \,^{+\,19}_{-\,21}$	$444 \pm 24 \,^{+\,9}_{-\,10}$	$445 \pm 24 \,^{+\,12}_{-\,13}$
[120]	$E_\ell > 1$	$450 \pm 27 \,^{+\,20}_{-\,22}$	$462 \pm 28 \,^{+\,9}_{-\,10}$	$462 \pm 28 \,^{+\,13}_{-\,13}$
[5]	HFLAV	$444 \pm 15 \,^{+\,21}_{-\,22}$	$452 \pm 15 \,^{+\,11}_{-\,14}$	$452 \pm 16 \,^{+\,15}_{-\,16}$

Hadronization uncertainties also impact the $|V_{ub}|$ determination. The theoretical expressions are valid at the parton level and do not incorporate any resonant structure (*e.g.* $\bar{B} \to \pi\ell\bar{\nu}_\ell$); this must be added to the simulated $\bar{B} \to X_u\ell\bar{\nu}_\ell$ event samples, since the detailed final state multiplicity and structure impacts the estimates of experimental acceptance and efficiency. The experiments have adopted procedures to input resonant structure while preserving the appropriate behavior in the kinematic variables (q^2, E_ℓ, m_X) averaged over the sample, but these prescriptions are *ad hoc*. The resulting uncertainties have been estimated to be $\sim$ 1-2% on $|V_{ub}|$.

All calculations yield compatible $|V_{ub}|$ values and similar error estimates. The arithmetic mean of the values and errors is $|V_{ub}| = (4.49 \pm 0.15_{\rm exp}\ ^{+0.16}_{-0.17\,\rm theo}) \times 10^{-3}$. However, for reasons discussed below, we believe there is an additional uncertainty due to model dependence that is not reflected in the HFLAV averages.

A new measurement [121] from BABAR based on the inclusive electron spectrum determines the partial branching fraction and $|V_{ub}|$ for $E_e > 0.8\,\text{GeV}$. This analysis shows clearly that the partial branching fraction itself has substantial model dependence when the kinematic acceptance includes regions dominated by $\bar{B} \to X_c\ell\bar{\nu}_\ell$ background. The values obtained for $|V_{ub}| \times 10^3$ are [121] $4.56 \pm 0.13\ ^{+0.28}_{-0.26}$ (BLNP), $3.96 \pm 0.10 \pm 0.17$ (GGOU) and $3.85 \pm 0.11\ ^{+0.08}_{-0.07}$ (DGE), where the first uncertainty is experimental and the second combines HQE parameter and theoretical uncertainties. The model dependence enters primarily through the partial branching fractions, and arises because the fit has sensitivity to $\bar{B} \to X_u\ell\bar{\nu}_\ell$ decays only in regions with good signal to noise (see Fig. 13 of Ref. 121). Each of the analyses shown in Table 94.1 was based on a partial branching fraction determined in a single model (i.e. the one used by that analysis when simulating $\bar{B} \to X_u\ell\bar{\nu}_\ell$ decays). The $|V_{ub}|$ value quoted by HFLAV for each model was derived from this unique partial branching fraction and the model-specific partial rate calculation. This translation from a single partial branching fraction into $|V_{ub}|$ values in different models suffers, in principle, from the difficulties made explicit in the recent BABAR measurement. The model dependence in the partial branching fraction is sensitive to how the model predictions compare in the restricted region with good signal-to-noise, not by how they compare when integrated over the full kinematic range used in the fit. This effect needs to be accounted for by the experiments; the published results are insufficient to determine it. To try to account for this model dependence, we add in quadrature to the $|V_{ub}|$ average an additional uncertainty whose size is estimated by taking the quadrature difference, averaged over the models, between the theory errors on $|V_{ub}|$ for the regions $m_X < 1.7\,\text{GeV}$ (good signal-to-noise) and $E_e > 1.0\,\text{GeV}$ (more inclusive, low signal-to-noise). With this addition, the inclusive $|V_{ub}|$ average is

$$|V_{ub}| = (4.49 \pm 0.15_{\rm exp}\ ^{+0.16}_{-0.17\,\rm theo} \pm 0.17_{\Delta\rm BF}) \times 10^{-3} \quad \text{(inclusive)}. \tag{94.29}$$

94.3.4. $|V_{ub}|$ *from exclusive decays* :

Exclusive charmless semileptonic decays offer a complementary means of determining $|V_{ub}|$. For the experiments, the specification of the final state provides better background rejection, but the branching fraction to a specific final state is typically only a few percent of that for inclusive decays. For theory, the calculation of the form factors for $\bar{B} \to X_u \ell \bar{\nu}_\ell$ decays is challenging, but brings in a different set of uncertainties from those encountered in inclusive decays. In this review we focus on $\bar{B} \to \pi \ell \bar{\nu}_\ell$, as it is the most promising decay mode for both experiment and theory. Measurements of other exclusive $\bar{B} \to X_u \ell \bar{\nu}_\ell$ decays can be found in Refs. [124–131].

94.3.5. $\bar{B} \to \pi \ell \bar{\nu}_\ell$ *form factor calculations* :

The relevant form factors for the decay $\bar{B} \to \pi \ell \bar{\nu}_\ell$ are usually defined as

$$\langle \pi(p_\pi)|V^\mu|B(p_B)\rangle = \tag{94.30}$$
$$f_+(q^2)\left[p_B^\mu + p_\pi^\mu - \frac{m_B^2 - m_\pi^2}{q^2} q^\mu\right] + f_0(q^2)\frac{m_B^2 - m_\pi^2}{q^2} q^\mu$$

in terms of which the rate becomes (in the limit $m_\ell \to 0$)

$$\frac{d\Gamma}{dq^2} = \frac{G_F^2 |V_{ub}|^2}{24\pi^3} |p_\pi|^3 |f_+(q^2)|^2, \tag{94.31}$$

where p_π is the pion momentum in the B meson rest frame.

Currently available non-perturbative methods for the calculation of the form factors include lattice QCD (LQCD) and light-cone sum rules (LCSR). The two methods are complementary in phase space, since the lattice calculation is restricted to the kinematical range of high momentum transfer q^2 to the leptons, while light-cone sum rules provide information near $q^2 = 0$. Interpolations between these two regions can be constrained by unitarity and analyticity.

Unquenched simulations for heavy-to-light decays, where quark loop effects are fully incorporated, are now standard, and have been performed by the Fermilab/MILC [132], the HPQCD [133] and the RBC/UKQCD [134] collaborations. The calculations differ in the way the b quark is simulated, with HPQCD using nonrelativistic QCD, and Fermilab/MILC and RBC/UKQCD using relativistic b quarks with the Fermilab and Columbia heavy-quark forumulations; they agree within the quoted errors. The result from Ref. 132 represents a significant improvement in precision. The form factor f_+ evaluated at $q^2 = 20\,\mathrm{GeV}^2$ has an estimated uncertainty of 3.4%, where the leading contribution is due to the chiral-continuum extrapolation fit, which includes statistical and heavy-quark discretization errors. However, the lattice simulations are restricted to the region of large q^2, i.e. the region $q^2_{\mathrm{max}} > q^2 \gtrsim 15\,\mathrm{GeV}^2$.

The extrapolation to small values of q^2 is performed using guidance from analyticity and unitarity. Making use of the heavy-quark limit, stringent constraints on the shape

of the form factor can be derived [135], and the conformal mapping of the kinematical variables onto the complex unit disc yields a rapidly converging series in the variable

$$z = \frac{\sqrt{t_+ - t_-} - \sqrt{t_+ - q^2}}{\sqrt{t_+ - t_-} + \sqrt{t_+ - q^2}}$$

where $t_\pm = (M_B \pm m_\pi)^2$. The use of lattice data in combination with experimental measurements of the differential decay rate provides a stringent constraint on the shape of the form factor in addition to precise determination of $|V_{ub}|$ [136].

Another established non-perturbative approach to obtain the form factors is through Light-Cone QCD Sum Rules (LCSR). The sum-rule approach provides an estimate for the product $f_B f_+(q^2)$, valid in the region $0 < q^2 \lesssim 12\ \mathrm{GeV}^2$. The determination of $f_+(q^2)$ itself requires knowledge of the decay constant f_B, which is usually obtained by replacing f_B by its two-point QCD (SVZ) sum rule [137] in terms of perturbative and condensate contributions. The advantage of this procedure is the approximate cancellation of various theoretical uncertainties in the ratio $(f_B f_+)/(f_B)$.

The LCSR for $f_B f_+$ is based on the light-cone OPE of the relevant vacuum-to-pion correlation function, calculated in full QCD at finite b-quark mass. The resulting expressions actually comprise a triple expansion: in the twist t of the operators near the light-cone, in α_s, and in the deviation of the pion distribution amplitudes from their asymptotic form, which is fixed from conformal symmetry. The sources of uncertainties in the LCSR calculation are discussed in Refs. 138 and 139; currently a total uncertainty slightly larger than 10% on $|V_{ub}|$ is obtained from a LCSR calculation of

$$\begin{aligned}\Delta\zeta(0, q^2_{max}) &= \frac{G_F^2}{24\pi^3} \int_0^{q^2_{max}} dq^2\, p_\pi^3 |f_+(q^2)|^2 \\ &= \frac{1}{|V_{ub}|^2 \tau_{B_0}} \int_0^{q^2_{max}} dq^2\, \frac{d\mathcal{B}(B \to \pi\ell\nu)}{dq^2}\end{aligned} \tag{94.32}$$

which gives [140]

$$\Delta\zeta(0, 12\,\mathrm{GeV}^2) = 4.59^{+1.00}_{-0.85}\,\mathrm{ps}^{-1}. \tag{94.33}$$

The recent calculation of two loop contributions to the LCSR [141] and the estimation of statistical correlations [142] results in only small changes to the central value and uncertainty.

94.3.6. $\bar{B} \to \pi\ell\bar{\nu}_\ell$ *measurements* :

The $\bar{B} \to \pi\ell\bar{\nu}_\ell$ measurements fall into two broad classes: untagged, in which case the reconstruction of the missing momentum of the event serves as an estimator for the unseen neutrino, and tagged, in which the second B meson in the event is fully reconstructed in either a hadronic or semileptonic decay mode. The tagged measurements have high and uniform acceptance and S/B as high as 10, but low statistical power. The untagged measurements have somewhat higher background (S/B < 1) and make slightly more restrictive kinematic cuts, but provide better precision on the q^2 dependence of the form factor.

Table 94.2: Total and partial branching fractions for $\bar{B}^0 \to \pi^+\ell^-\bar{\nu}_\ell$. B-tagged analyses are indicated (SL *for semileptonic*, Had *for hadronic*). The first uncertainty listed is from statistics, the second from systematics. Measurements of $\mathcal{B}(B^- \to \pi^0\ell^-\bar{\nu}_\ell)$ have been multiplied by a factor $2\tau_{B^0}/\tau_{B^+}$ to obtain the values below.

	$\mathcal{B}\times 10^4$	$\mathcal{B}(q^2 > 16) \times 10^4\,\mathrm{GeV}^2$
CLEO π^+, π^0 [129]	$1.38 \pm 0.15 \pm 0.11$	$0.41 \pm 0.08 \pm 0.04$
BABAR π^+, π^0 [130]	$1.41 \pm 0.05 \pm 0.08$	$0.32 \pm 0.02 \pm 0.03$
BABAR π^+ [131]	$1.44 \pm 0.04 \pm 0.06$	$0.37 \pm 0.02 \pm 0.02$
Belle π^+, π^0 [143]	$1.48 \pm 0.04 \pm 0.07$	$0.40 \pm 0.02 \pm 0.02$
Belle SL π^+ [144]	$1.41 \pm 0.19 \pm 0.15$	$0.37 \pm 0.10 \pm 0.04$
Belle SL π^0 [144]	$1.41 \pm 0.26 \pm 0.15$	$0.37 \pm 0.15 \pm 0.04$
Belle Had π^+ [124]	$1.49 \pm 0.09 \pm 0.07$	$0.45 \pm 0.05 \pm 0.02$
Belle Had π^0 [124]	$1.48 \pm 0.15 \pm 0.08$	$0.36 \pm 0.07 \pm 0.02$
BABAR SL π^+ [145]	$1.38 \pm 0.21 \pm 0.08$	$0.46 \pm 0.13 \pm 0.03$
BABAR SL π^0 [145]	$1.78 \pm 0.28 \pm 0.15$	$0.44 \pm 0.17 \pm 0.06$
BABAR Had π^+ [146]	$1.07 \pm 0.27 \pm 0.19$	$0.65 \pm 0.20 \pm 0.13$
BABAR Had π^0 [146]	$1.52 \pm 0.41 \pm 0.30$	$0.48 \pm 0.22 \pm 0.12$
Average [147]	$1.45 \pm 0.02 \pm 0.04$	$0.38 \pm 0.01 \pm 0.01$

CLEO has analyzed $\bar{B} \to \pi\ell\bar{\nu}_\ell$ and $\bar{B} \to \rho\ell\bar{\nu}_\ell$ using an untagged analysis [129]. Similar analyses have been done at BABAR [130,131] and Belle [143]. The leading systematic uncertainties in the untagged $\bar{B} \to \pi\ell\bar{\nu}_\ell$ analyses are associated with modeling the missing momentum reconstruction, with backgrounds from $\bar{B} \to X_u\ell\bar{\nu}_\ell$ decays and $e^+e^- \to q\bar{q}$ continuum events, and with varying the form factor used to model $\bar{B} \to \rho\ell\bar{\nu}_\ell$ decays. The values obtained for the full and partial branching fractions are listed in Table 94.2 above the horizontal line.

Analyses [144,145] based on reconstructing a B in the $\bar{D}^{(*)}\ell^+\nu_\ell$ decay mode and looking for a $\bar{B} \to \pi\ell\bar{\nu}_\ell$ or $\bar{B} \to \rho\ell\bar{\nu}_\ell$ decay amongst the remaining particles in the event

make use of the fact that the B and $\bar{B}$ are back-to-back in the $\Upsilon(4S)$ frame to construct a discriminant variable that provides a signal-to-noise ratio above unity for all q^2 bins. A related technique was discussed in Ref. 148. BABAR [145] and Belle [124] have also used their samples of B mesons reconstructed in hadronic decay modes to measure exclusive charmless semileptonic decays, resulting in very clean but small samples. The corresponding full and partial branching fractions are given in Table 94.2. The averages [147] take account of correlations and common systematic uncertainties, and have $p(\chi^2) > 0.5$ in each case.

$|V_{ub}|$ can be obtained from the average $\bar{B} \to \pi\ell\bar{\nu}_\ell$ branching fraction and the measured q^2 spectrum. Fits to the q^2 spectrum using a theoretically motivated parameterization (e.g. "BCL" from Ref. 149) remove most of the model dependence from theoretical uncertainties in the shape of the spectrum. The most sensitive method for determining $|V_{ub}|$ from $\bar{B} \to \pi\ell\bar{\nu}_\ell$ decays employs a simultaneous fit [5,132,150] to measured experimental partial rates and lattice points versus q^2 (or z) to determine $|V_{ub}|$ and the first few coefficients of the expansion of the form factor in z. We quote the result from Ref. 5, which uses as experimental input an average of the measurements in Refs. [124,130,131,143] and an average [151] of the LQCD input from Refs. 132 and 134 and finds

$$|V_{ub}| = (3.70 \pm 0.10 \pm 0.12\,) \times 10^{-3} \quad \text{(exclusive)}, \tag{94.34}$$

where the first uncertainty is experimental and the second is from theory. Adding an additional constraint using input [152] from LCSR gives [5] $|V_{ub}| = (3.67 \pm 0.09 \pm 0.12\,) \times 10^{-3}$ (exclusive, LQCD + LCSR).

94.4. Semileptonic b-baryon decays & determination of $|V_{ub}|/|V_{cb}|$

Summary: A significant sample of Λ_b^0 baryons is available at the LHCb experiment, and methods have been developed to study their semileptonic decays. Both $\Lambda_b^0 \to p\mu\bar{\nu}$ and $\Lambda_b^0 \to \Lambda_c^+\mu\bar{\nu}$ decays have been measured at LHCb, and the ratio of branching fractions to these two decay modes is used to determine the ratio $|V_{ub}/V_{cb}|$. Averaging the LHCb determination with those obtained from inclusive and exclusive B meson decays, we find

$$|V_{ub}|/|V_{cb}| = 0.092 \pm 0.008 \quad \text{(average)}$$

where the average has $p(\chi^2) = 0.9\%$ and the uncertainty has been scaled by a factor $\sqrt{\chi^2/2} = 2.2$. In light of the poor consistency of the three determinations considered, the average should be treated with caution.

94.4.1. $\Lambda_b^0 \to \Lambda_c^+\mu\bar{\nu}$ and $\Lambda_b^0 \to p\mu\bar{\nu}$:

The $\Lambda_b^0 \to \Lambda_c^+$ and $\Lambda_b^0 \to p$ semileptonic transitions are described in terms of six form factors each. The three form factors corresponding to the vector current can be defined as [153]

$$\langle F(p',s')|\bar{q}\,\gamma_\mu\,b|\Lambda_b^0(p,s)\rangle = \bar{u}_F(p',s')\left\{ f_0(q^2)\,(M_{\Lambda_b^0} - m_F)\,\frac{q_\mu}{q^2}\right.$$

$$+f_+(q^2)\,\frac{M_{\Lambda_b^0}+m_F}{s_+}\left(p_\mu+p'_\mu-\frac{q_\mu}{q^2}\,(M^2_{\Lambda_b^0}-m_F^2)\right)$$
$$+f_\perp(q^2)\left(\gamma_\mu-\frac{2m_F}{s_+}\,p_\mu-\frac{2M_{\Lambda_b^0}}{s_+}\,p'_\mu\right)\Bigg\}\,u_{\Lambda_b^0}(p,s)\,, \tag{94.35}$$

where $F = p$ or Λ_c^+ and where we define $s_\pm = (M_{\Lambda_b^0} \pm m_F)^2 - q^2$. At vanishing momentum transfer, $q^2 \to 0$, the kinematic constraint $f_0(0) = f_+(0)$ holds. The form factors are defined in such a way that they correspond to time-like (scalar), longitudinal and transverse polarization with respect to the momentum-transfer q^μ for f_0, f_+ and $f_\perp$, respectively. Furthermore we have chosen the normalization in such a way that for $f_0, f_+, f_\perp \to 1$ one recovers the expression for point-like baryons.

Likewise, the expression for the axial-vector current is

$$\begin{aligned}\langle F(p',s')|\bar q\,\gamma_\mu\gamma_5\,b|\Lambda_b^0(p,s)\rangle = &-\bar u_F(p',s')\gamma_5\\ &\Big\{g_0(q^2)\,(M_{\Lambda_b^0}+m_F)\,\frac{q_\mu}{q^2}\\ &+g_+(q^2)\,\frac{M_{\Lambda_b^0}-m_F}{s_-}\left(p_\mu+p'_\mu-\frac{q_\mu}{q^2}\,(M^2_{\Lambda_b^0}-m_F^2)\right)\\ &+g_\perp(q^2)\left(\gamma_\mu+\frac{2m_F}{s_-}\,p_\mu-\frac{2M_{\Lambda_b^0}}{s_-}\,p'_\mu\right)\Big\}\,u_{\Lambda_b^0}(p,s)\,,\end{aligned} \tag{94.36}$$

with the kinematic constraint $g_0(0) = g_+(0)$ at $q^2 \to 0$.

The form factors have been discussed in the heavy quark limit; assuming both b and c as heavy, all the form factors f_i and g_i turn out to be identical [153]

$$f_0 = f_+ = f_\perp = g_0 = g_+ = g_\perp = \xi_B \tag{94.37}$$

and equal to the Isgur Wise function ξ_B for baryons. In the limit of a light baryon in the final state, the number of independent form factors is still reduced to two through the heavy quark symmetries of the Λ_b^0. It should be noted that the $\Lambda_b^0 \to (p/\Lambda_c^+)\mu\nu$ decay rates peak at high q^2, which facilitates both lattice QCD calculations and experimental measurements.

The form factors for Λ_b^0 decays have been studied on the lattice [154]. Based on these results the differential rates for both $\Lambda_b^0 \to \Lambda_c^+\mu\bar\nu$ as well as for $\Lambda_b^0 \to p\mu\bar\nu$ can be predicted in the full phase space. In particular, for the experimentally interesting region they find the ratio of decay rates to be [154]

$$\frac{\mathcal{B}(\Lambda_b^0 \to p\mu\bar\nu)_{q^2>15\ \mathrm{GeV}^{\,2}}}{\mathcal{B}(\Lambda_b^0 \to \Lambda_c^+\mu\bar\nu)_{q^2>7\ \mathrm{GeV}^{\,2}}} = (1.471 \pm 0.095 \pm 0.109)\left|\frac{V_{ub}}{V_{cb}}\right|^2 \tag{94.38}$$

where the first uncertainty is statistical and the second, systematic.

94.4.2. *Measurements at LHCb* :

The LHCb experiment has measured the branching fractions of the semileptonic decays $\Lambda_b^0 \to \Lambda_c^+ \mu\bar{\nu}$ and $\Lambda_b^0 \to p\mu\bar{\nu}$, from which they determine $|V_{ub}|/|V_{cb}|$. This is the first such determination at a hadron collider, the first to use a b baryon decay, and the first observation of $\Lambda_b^0 \to p\mu\bar{\nu}$. Excellent vertex resolution allows the $p\mu$ and production vertices to be separated, which permits the calculation of the transverse momentum $p_\perp$ of the $p\mu$ pair relative to the Λ_b^0 flight direction. The corrected mass, $m_{\rm corr} = \sqrt{p_\perp^2 + m_{p\mu}^2} + p_\perp$, peaks at the Λ_b^0 mass for signal decays and provides good discrimination against background combinations. The topologically similar decay $\Lambda_b^0 \to \Lambda_c^+ \mu\bar{\nu}$ is also measured, which eliminates the need to know the production cross-section or absolute efficiencies. Using vertex and Λ_b^0 mass constraints, q^2 can be determined up to a two-fold ambiguity. The LHCb analysis requires both solutions to be in the high q^2 region to minimise contamination from the low q^2 region. Their result [155], rescaled [5] to take into account the recent branching fraction measurement [156] $\mathcal{B}(\Lambda_c^+ \to pK^-\pi^+) = (5.84 \pm 0.27 \pm 0.23)\%$, is

$$\frac{\mathcal{B}(\Lambda_b^0 \to p\mu\bar{\nu})_{q^2>15{\rm GeV}^2}}{\mathcal{B}(\Lambda_b^0 \to \Lambda_c^+ \mu\bar{\nu})_{q^2>7{\rm GeV}^2}} = (0.95 \pm 0.04 \pm 0.07) \times 10^{-2} \quad . \tag{94.39}$$

The largest systematic uncertainty is from the measured $\mathcal{B}(\Lambda_c^+ \to pK^-\pi^+)$; uncertainties due to trigger, tracking and the Λ_c^+ selection efficiency are each about 3%.

A recent LHCb analysis [157] measures the normalized q^2 spectrum and finds good agreement with the shape calculated on the lattice [154].

94.4.3. *The ratio $|V_{ub}|/|V_{cb}|$* :

The ratio of matrix elements, $|V_{ub}|/|V_{cb}|$, is often required when testing the compatibility of a set of measurements with theoretical predictions. It can be determined from the ratio of branching fractions measured by the LHCb experiment, quoted in the previous section. It can also be calculated based on the $|V_{ub}|$ and $|V_{cb}|$ values quoted earlier in this review.

As previously noted, the decay rate for $\Lambda_b^0 \to p\mu\bar{\nu}$ peaks at high q^2 where the calculation of the associated form factors using lattice QCD is under good control. Using the measured ratio from Eq. (94.39) along with the calculations of Ref. 154 results in [5]

$$|V_{ub}|/|V_{cb}| = 0.080 \pm 0.004 \pm 0.004 \quad \text{(LHCb)}. \tag{94.40}$$

where the first uncertainty is experimental and the second is from the LQCD calculation.

Given the similarities in the theoretical frameworks used for charmed and charmless decays, we choose to quote the ratio $|V_{ub}|/|V_{cb}|$ separately for inclusive and exclusive decays:

$$|V_{ub}|/|V_{cb}| = 0.107 \pm 0.007 \quad \text{(inclusive)}, \tag{94.41}$$

$$|V_{ub}|/|V_{cb}| = 0.088 \pm 0.006 \quad \text{(exclusive)}. \tag{94.42}$$

We average these values, along with the result in Eq. (94.40), weighting by relative errors. The average has $p(\chi^2) = 0.9\%$, so we scale the uncertainty by a factor $\sqrt{\chi^2/2} = 2.2$ to find

$$|V_{ub}|/|V_{cb}| = 0.092 \pm 0.008 \quad \text{(average)}. \tag{94.43}$$

94.5. Semitauonic decays

Summary: Semileptonic decays to third-generation leptons provide sensitivity to non-Standard Model amplitudes, such as from a charged Higgs boson [158]. The ratios of branching fractions of semileptonic decays involving tau leptons to those involving e/μ, $\mathcal{R}_{D^{(*)}} \equiv \mathcal{B}(\bar{B} \to D^{(*)}\tau\bar{\nu}_\tau)/\mathcal{B}(\bar{B} \to D^{(*)}\ell\bar{\nu}_\ell)$, are predicted with good precision in the Standard Model [34,159–163]. For $\mathcal{R}_D$ the most precise value comes from a fit to lattice and experimental data [163], while for $\mathcal{R}_{D^*}$ we use a calculation [161] based on the heavy quark expansion, combined with the measurements for $\bar{B} \to D^*\ell\bar{\nu}_\ell$

$$\begin{aligned} \mathcal{R}_D^{\rm SM} &= 0.299 \pm 0.003 \ , \\ \mathcal{R}_{D^*}^{\rm SM} &= 0.252 \pm 0.003 \ . \end{aligned} \tag{94.44}$$

Measurements [164–170] of these ratios yield higher values; averaging B-tagged measurements of $\mathcal{R}_D$ and $\mathcal{R}_{D^*}$ at the $\Upsilon(4S)$ and the LHCb measurements of $\mathcal{R}_{D^*}$ yields [171]

$$\begin{aligned} \mathcal{R}_D^{\rm meas} &= 0.407 \pm 0.039 \pm 0.024 \\ \mathcal{R}_{D^*}^{\rm meas} &= 0.304 \pm 0.013 \pm 0.007 \end{aligned} \tag{94.45}$$

with a linear correlation of -0.20. These values exceed Standard Model predictions by 2.3σ and 3.4σ, respectively. A variety of new physics models have been proposed [158,172–178] to explain this excess. Most models proposed to explain the semitauonic decays have very little impact on semileptonic decays involving muons or electrons, so they do not significantly modify the $|V_{ub}|$ or $|V_{cb}|$ determinations discussed previously in this review.

94.5.1. *Sensitivity of $\bar{B} \to D^{(*)}\tau\bar{\nu}_\tau$ to additional amplitudes* :

In addition to the helicity amplitudes present for decays to $e\bar{\nu}_e$ and $\mu\bar{\nu}_\mu$, decays proceeding through $\tau\bar{\nu}_\tau$ include a scalar amplitude H_s. The differential decay rate is given by [179]

$$\begin{aligned} \frac{d\Gamma}{dq^2} = \frac{G_F^2\,|V_{cb}|^2\,|\mathbf{p}^*_{D^{(*)}}|q^2}{96\pi^3 m_B^2}\left(1-\frac{m_\tau^2}{q^2}\right)^2 \\ \left[(|H_+|^2+|H_-|^2+|H_0|^2)\left(1+\frac{m_\tau^2}{2q^2}\right)+\frac{3m_\tau^2}{2q^2}|H_s|^2\right], \end{aligned} \tag{94.46}$$

where $|\mathbf{p}^*_{D^{(*)}}|$ is the 3-momentum of the $D^{(*)}$ in the $\bar{B}$ rest frame and the helicity amplitudes H depend on the four-momentum transfer q^2. All four helicity amplitudes

contribute to $\bar{B} \to D^* \tau \bar{\nu}_\tau$, while only H_0 and H_s contribute to $\bar{B} \to D \tau \bar{\nu}_\tau$; as a result, new physics contributions tend to produce larger effects in the latter mode.

The (semi)-leptonic B decays into a τ lepton provide a stringent test of the two-Higgs doublet model of type II (2HDMII), i.e. where the two Higgs doublets couple separately to up- and down-type quarks. This is also of relevance for Supersymmetry, since this corresponds to the Higgs sector of any commonly used supersymmetric model. These models involve additional charged scalar particles, which contribute at tree level to the (semi)-leptonic B decays into a τ. The distinct feature of the 2HDMII is that the contributions of the charged scalars scale as $m_\tau^2/m_{H^+}^2$, since the couplings to the charged Higgs particles are proportional to the mass of the lepton. As a consequence, one may expect visible effects in decays into a τ, but only small effects for decays into e and μ.

As discussed in the next section, the 2HDMII does not describe the observations any better than the Standard Model. To achieve a better description one has to extend the analysis to other models, where the scaling of the new contributions with the lepton mass is different.

94.5.2. *Measurement of $\mathcal{R}_{D^{(*)}}$* :

$\bar{B} \to D^{(*)} \tau \bar{\nu}_\tau$ decays have been studied at the $\Upsilon(4S)$ resonance and in pp collisions. At the $\Upsilon(4S)$, the experimental signature consists of a D or D^* meson, an electron or muon (denoted here by ℓ) from the decay $\tau \to \ell \nu_\tau \overline{\nu}_\ell$, a fully-reconstructed decay of the second B meson in the event, and multiple missing neutrinos. The analyses that use hadronic B tags separate signal decays from $\bar{B} \to D^{(*)} \ell \bar{\nu}_\ell$ decays using the lepton momentum and the measured missing mass squared; decays with only a single missing neutrino peak sharply at zero in this variable, while the signal is spread out to positive values. When a semileptonic B tag is used, the main discrimination between signal and $\bar{B} \to D^{(*)} \ell \bar{\nu}_\ell$ decays comes from the calorimeter energy that is unassociated with any particle used in the reconstruction of the B meson candidates and the cosine of the angle between the $D^* \ell$ system and its parent B meson, which is calculated under the assumption that only one particle (a neutrino) is missing. In both these approaches, background from $\bar{B} \to D^{**} \ell \bar{\nu}_\ell$ decays with one or more unreconstructed particles is harder to separate from signal, as is background from $\bar{B} \to D^{(*)} H_{\bar{c}} X$ (where $H_{\bar{c}}$ is a hadron containing a $\bar{c}$ quark) decays. The leading sources of systematic uncertainty are due to the limited size of simulation samples used in constructing the PDFs, the composition of the D^{**} states, efficiency corrections, and cross-feed (swapping soft particles between the signal and tag B).

A recent measurement [168] uses hadronic B tags and τ^+ decays to $\pi^+ \bar{\nu}_\tau$ or $\rho^+ \bar{\nu}_\tau$ to measure $\mathcal{R}_{D^*}$ and the polarization of the τ^+ lepton. The main discriminant variables are the measured missing mass squared and the unassociated calorimeter energy. This measurement provides the first determination of the τ polarization in the $\bar{B} \to D^* \tau \bar{\nu}_\tau$ decay, $\mathcal{P}(D^*) = -0.38 \pm 0.51\ ^{+0.21}_{-0.16}$, compatible with the standard model expectation [180], -0.497 ± 0.013. The main uncertainties on the $\mathcal{R}_{D^*}$ measurement come from the composition of the hadronic B background and from modeling of semileptonic B decays and mis-reconstructed D^* mesons.

The LHCb experiment has studied the decay $\bar{B} \to D^{*+} \tau \bar{\nu}_\tau$ with $D^{*+} \to D^0 \pi^+$, $D^0 \to K^- \pi^+$ and $\tau \to \mu \nu_\tau \overline{\nu}_\mu$ in pp collisions. Their analysis [169] takes advantage of the

measurable flight lengths of b and c hadrons and τ leptons. A multivariate discriminant is used to select decays where no additional charged particles are consistent with coming from the signal decay vertices. The separation between the primary and B decay vertices is used to calculate the momentum of the B decay products transverse to the B flight direction. The longitudinal component of the B momentum can be estimated based on the visible decay products; this allows a determination of the B rest frame, with modest resolution, and enables the calculation of the same discrimination variables available at the e^+e^- B factories. The (rest frame) muon energy, missing mass-squared and q^2 are used in a 3-d fit. The leading sources of systematic uncertainty are due to the size of the simulation sample used in constructing the fit templates, the shape of the muon misidentification template, and uncertainties in modelling the background from $\bar{B} \to D^{**}\ell\bar{\nu}_\ell$ and $\bar{B} \to D^{(*)}H_{\bar{c}}X$ decays. The most recent LHCb preliminary result [170] on $\mathcal{R}_{D^*}$ uses three-prong decays that take advantage of their excellent vertex resolution.

Measurements from BABAR [164,165], Belle [166–168] and LHCb [169,170] result in values for $\mathcal{R}_D$ and $\mathcal{R}_{D^*}$ that exceed Standard Model predictions. Table 94.3 lists these values and their average. The simultaneous measurements of $\mathcal{R}_D$ and $\mathcal{R}_{D^*}$ have linear correlation coefficients of -0.27 (BABAR) and -0.49 (Belle); the $\mathcal{R}_D$ and $\mathcal{R}_{D^*}$ averages have a correlation of -0.20. Two untagged Belle measurements [181,182] are subject to larger systematic uncertainties; they are not included in the average. All three experiments assume the Standard Model kinematic distributions for $\bar{B} \to D^{(*)}\tau\bar{\nu}_\tau$ in their determinations of the branching fraction ratios.

Table 94.3: Measurements of $\mathcal{R}_D$ and $\mathcal{R}_{D^*}$ and their averages [171]. The correlation between the $\mathcal{R}_D$ and $\mathcal{R}_{D^*}$ averages is -0.20.

		$\mathcal{R}_D \times 10^2$	$\mathcal{R}_{D^*} \times 10^2$
BABAR [165]	B^0, B^+	$44.0 \pm 5.8 \pm 4.2$	$33.2 \pm 2.4 \pm 1.8$
Belle [166]	B^0, B^+	$37.5 \pm 6.4 \pm 2.6$	$29.3 \pm 3.8 \pm 1.5$
Belle [167]	B^0, B^+		$30.2 \pm 3.0 \pm 1.1$
Belle [168]	B^0, B^+		$27.0 \pm 3.5 \,^{+\,2.8}_{-\,2.5}$
LHCb [169]	B^0		$33.6 \pm 2.7 \pm 3.0$
LHCb [170]	B^0		$28.5 \pm 1.9 \pm 2.9$
Average	B^0, B^+	$40.7 \pm 3.9 \pm 2.4$	$30.4 \pm 1.3 \pm 0.7$

The tension between the SM prediction and the measurements is at the level of 2.3σ (R_D) and 3.4σ (R_{D^*}); if one considers these deviations together the significance rises to 4.1σ. This motivates speculation on possible new physics contributions. It is striking that an interpretation in terms of the 2HDMII seems to be ruled out by the data. Fig. 94.1 shows that the interpretation of the deviation of $\mathcal{R}_D$ in terms of the 2HDMII requires vastly different values of the relevant parameter $\tan\beta/m_{H^+}$ than for $\mathcal{R}_{D^*}$, excluding this possibility. The BABAR [165] and Belle [166] analyses use kinematical

distributions from the 2HDMII when comparing the compatibility of their measurements with predictions; this is why the band in Fig. 94.1 corresponding to the measurement varies with $\tan\beta/m_{H^+}$. In general, new physics contributions with a different operator structure to the SM could modify $R_{D^{(*)}}$ from the measured values, and could have a different effect in different experiments.

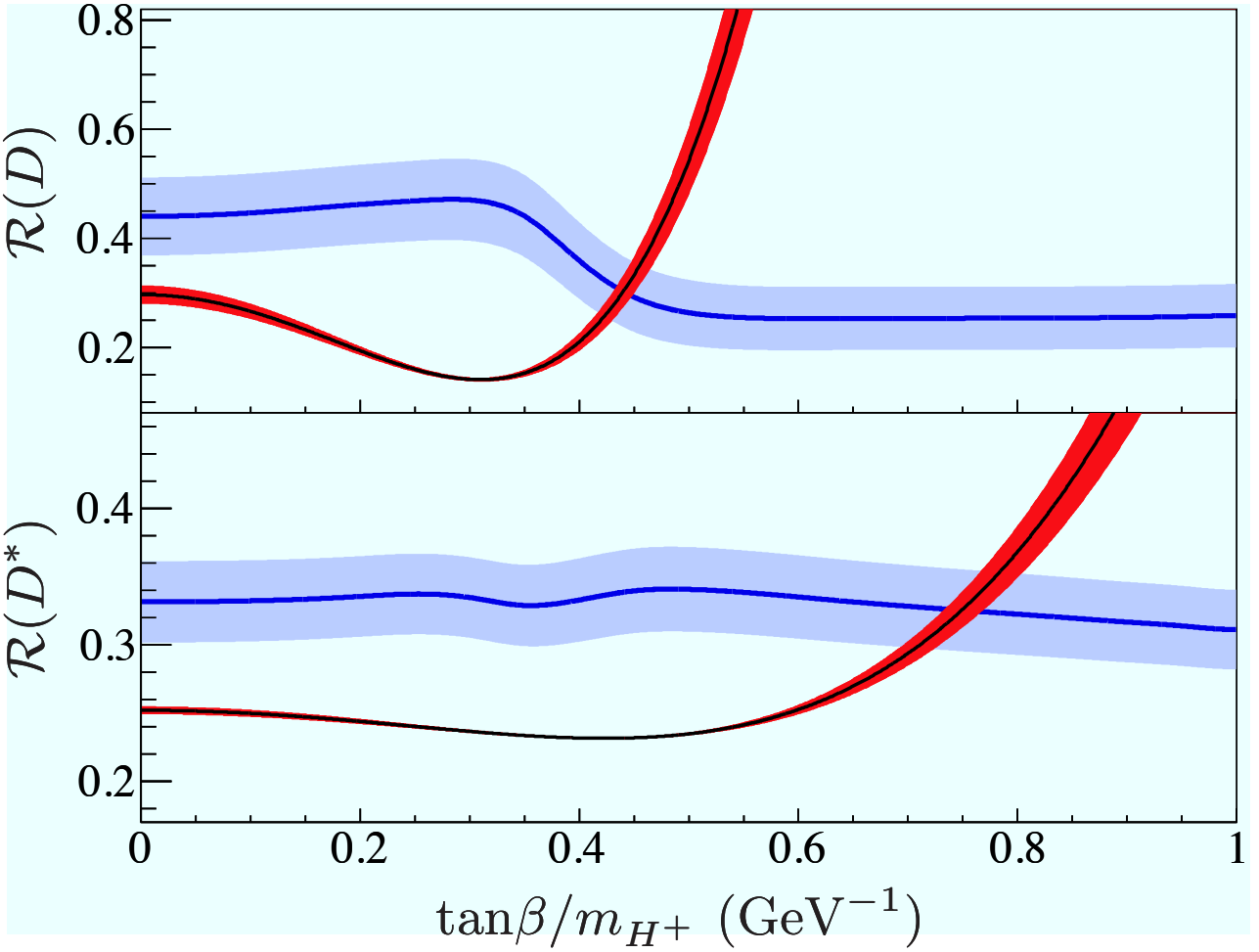

Figure 94.1: The $\mathcal{R}_{D^{(*)}}$ measured in Ref. 165 (thick bands) along with expectations in the 2HDMII (thin bands) as a function of $\tan\beta/m_{H^+}$.

A more general approach has been formulated in Ref. 174 on the basis of an effective field theory. Assuming lepton-flavour-universality-violating operators of dimension six and eight, the coefficients of these operators can be fitted to the observed values. Although a detailed analysis along these lines requires more data on related decays (such as $B \to \pi\tau\bar{\nu}$, for which only a limit [183] exists at present), there are indications that the tension in $\mathcal{R}_{D^{(*)}}$ cannot be explained by a minimally flavor-violating scenario with only left-handed interactions; a better fit is obtained once right-handed and scalar currents are included.

94.6. Conclusion

The study of semileptonic B meson decays continues to be an active area for both theory and experiment. The application of HQE calculations to inclusive decays is mature, and fits to moments of $\bar{B} \to X_c \ell \bar{\nu}_\ell$ decays provide precise values for $|V_{cb}|$ and, in conjunction with input on m_c or from $B \to X_s \gamma$ decays, provide precise and consistent values for m_b.

The determination of $|V_{ub}|$ from inclusive $\bar{B} \to X_u \ell \bar{\nu}_\ell$ decays is based on multiple calculational approaches and independent measurements over a variety of kinematic regions, all of which provide consistent results. Further progress in this area is possible, but will require better theoretical control over higher-order terms, improved experimental knowledge of the $\bar{B} \to X_c \ell \bar{\nu}_\ell$ background and improvements to the modeling of the $\bar{B} \to X_u \ell \bar{\nu}_\ell$ signal distributions.

In both $b \to u$ and $b \to c$ exclusive channels there has been significant recent progress in lattice-QCD calculations, resulting in improved precision on both $|V_{ub}|$ and $|V_{cb}|$. These calculations now provide information on the form factors well away from the high q^2 region, allowing better use of experimental data. Projections for future uncertainties from lattice calculations can be found in Ref. 184.

The values from the inclusive and exclusive determinations of $|V_{ub}|$ are only marginally consistent. This is a long-standing puzzle, and the new measurement of $|V_{ub}|/|V_{cb}|$ from LHCb based on Λ_b^0 decays does not simplify the picture. The exclusive determination of $|V_{cb}|$ is currently under discussion to clarify the impact of different form-factor parameterizations.

Both $|V_{cb}|$ and $|V_{ub}|$ are indispensable inputs into unitarity triangle fits. In particular, knowing $|V_{ub}|$ with good precision allows a test of CKM unitarity in a most direct way, by comparing the length of the $|V_{ub}|$ side of the unitarity triangle with the measurement of $\sin(2\beta)$. This comparison of a "tree" process ($b \to u$) with a "loop-induced" process ($B^0 - \bar{B}^0$ mixing) provides sensitivity to possible contributions from new physics.

The observation of semileptonic decays into τ leptons has opened a new window to the physics of the third generation. The measurements indicate a tension between the data and the Standard Model prediction, which could be a hint for new physics, manifesting itself as a violation of lepton universality beyond the standard-model couplings to the Higgs. However, the most prominent and simplest candidate, the 2HDMII, cannot explain the current data. More general ansatzes fit the data, but do not provide deeper insight until measurements of related processes (such as $B \to \pi \tau \bar{\nu}$) are available. In addition, searches for a non-standard model lepton universality violation in the light lepton sector would complement the measurements of semi-tauonic decays.

The authors would like to acknowledge helpful input from M. Artuso, F. Bernlochner, G. Ricciardi and P. Urquijo.

References:

1. See R. Kowalewski and T. Mannel in C. Patrignani *et al.* (Particle Data Group), Chin. Phys. C **40**, 100001 (2016).
2. See "Heavy-Quark and Soft-Collinear Effective Theory" by C.W. Bauer and M. Neubert in this *Review*.

3. See "Lattice Quantum Chromodynamics" by S. Hashimoto, J. Laiho, and S.R. Sharpe in this *Review*.
4. See "Production and Decay of b-Flavored Hadrons" by P. Eerola, M. Kreps and Y. Kwon in this *Review*.
5. Y. Amhis *et al.* (HFLAV), `arXiv:1612.07233`, to appear in Eur. Phys. J. **C**.
6. N. Isgur and M.B. Wise, Phys. Lett. **B232**, 113 (1989); *ibid.* **B237**, 527 (1990).
7. M.A. Shifman and M.B. Voloshin, Sov. J. Nucl. Phys. **47**, 511 (1988) [Yad. Fiz. **47**, 801 (1988)].
8. M.E. Luke, Phys. Lett. **B252**, 447 (1990).
9. A.V. Manohar and M.B. Wise, Camb. Monogr. Part. Phys. Nucl. Phys. Cosmol. **10**, 1 (2000);
   H. Georgi, Phys. Lett. **B240**, 447 (1990);
   A.F. Falk *et al.*, Nucl. Phys. **B343**, 1 (1990);
   E. Eichten and B. Hill, Phys. Lett. **B234**, 511 (1990).
10. A. Sirlin, Nucl. Phys. **B196**, 83 (1982).
11. J.A. Bailey *et al.* [Fermilab Lattice and MILC Collab.], Phys. Rev. **D89**, 114504 (2014).
12. J. Harrison, C. Davies and M. Wingate, PoS LATTICE **2016**, 287 (2017).
13. C.G. Boyd, B. Grinstein, and R.F. Lebed, Phys. Rev. Lett. **74**, 4603 (1995); *ibid.*Phys. Rev. **D56**, 6895 (1997); B. Grinstein and A. Kobach, Phys. Lett. **B771**, 359 (2017).
14. I. Caprini *et al.*, Nucl. Phys. **B530**, 153 (1998).
15. B. Grinstein and A. Kobach, Phys. Lett. **B771**, 359 (2017).
16. D. Bigi, P. Gambino and S. Schacht, Phys. Lett. **B769**, 441 (2017).
17. A. Czarnecki and K. Melnikov, Nucl. Phys. **B505**, 65 (1997).
18. I.I.Y. Bigi *et al.*, Phys. Rev. **D52**, 196 (1995).
19. A. Kapustin *et al.*, Phys. Lett. **B375**, 327 (1996).
20. P. Gambino, T. Mannel, and N. Uraltsev, Phys. Rev. **D81**, 113002 (2010).
21. P. Gambino, T. Mannel, and N. Uraltsev, JHEP **1210**, 169 (2012).
22. D. Buskulic *et al.* (ALEPH Collab.), Phys. Lett. **B395**, 373 (1997).
23. G. Abbiendi *et al.* (OPAL Collab.), Phys. Lett. **B482**, 15 (2000).
24. P. Abreu *et al.* (DELPHI Collab.), Phys. Lett. **B510**, 55 (2001).
25. J. Abdallah *et al.* (DELPHI Collab.), Eur. Phys. J. **C33**, 213 (2004).
26. N.E. Adam *et al.* (CLEO Collab.), Phys. Rev. **D67**, 032001 (2003).
27. B. Aubert *et al.* (BABAR Collab.), Phys. Rev. **D77**, 032002 (2008).
28. B. Aubert *et al.* (BABAR Collab.), Phys. Rev. Lett. **100**, 231803 (2008).
29. B. Aubert *et al.* (BABAR Collab.), Phys. Rev. **D79**, 012002 (2009).
30. W. Dungel *et al.* (Belle Collab.), Phys. Rev. **D82**, 112007 (2010).
31. A. Abdesselam *et al.* (Belle Collab.), `arXiv:1702.01521`.
32. F. U. Bernlochner *et al.*, `arXiv:1708.07134`.
33. C. Bourrely, L. Lellouch, and I. Caprini, Phys. Rev. **D79**, 013008 (2012).
34. J. Bailey *et al.* [Fermilab Lattice and MILC Collab.], Phys. Rev. **D92**, 034506 (2015).
35. B. Aubert *et al.* (BABAR Collab.), Phys. Rev. Lett. **104**, 011802 (2010).

36. R. Glattauer *et al.* (Belle Collab.), Phys. Rev. **D93**, 032006 (2016).
37. A.V. Manohar and M.B. Wise, Phys. Rev. **D49**, 1310 (1994).
38. I.I.Y. Bigi *et al.*, Phys. Rev. Lett. **71**, 496 (1993); Phys. Lett. **B323**, 408 (1994).
39. D. Benson *et al.*, Nucl. Phys. **B665**, 367 (2003).
40. M. Gremm and A. Kapustin, Phys. Rev. **D55**, 6924 (1997).
41. B.M. Dassinger, T. Mannel, and S. Turczyk, JHEP **0703**, 087 (2007).
42. I.I. Bigi, N. Uraltsev, and R. Zwicky, Eur. Phys. J. **C50**, 539 (2007).
43. T. Mannel, S. Turczyk, and N. Uraltsev, JHEP **1011**, 109 (2010).
44. A. Pak and A. Czarnecki, Phys. Rev. **D78**, 114015 (2008).
45. S. Biswas and K. Melnikov, JHEP **1002**, 089 (2010).
46. P. Gambino, JHEP **1109**, 055 (2011).
47. P. Gambino and N. Uraltsev, Eur. Phys. J. **C34**, 181 (2004).
48. V. Aquila *et al.*, Nucl. Phys. **B719**, 77 (2005).
49. T. Becher, H. Boos, and E. Lunghi, JHEP **0712**, 062 (2007).
50. A. Alberti *et al.*, Nucl. Phys. **B870**, 16 (2013).
51. A. Alberti *et al.*, JHEP **1401**, 147 (2014).
52. T. Mannel, A.A. Pivovarov, and D. Rosenthal, Phys. Rev. **D92**, 054025 (2015).
53. C. Breidenbach *et al.*, Phys. Rev. **D78**, 014022 (2008).
54. I. Bigi *et al.*, JHEP **1004**, 073 (2010).
55. I. I. Y. Bigi, M. A. Shifman, N. G. Uraltsev and A. I. Vainshtein, Phys. Rev. D **50**, 2234 (1994).
56. A.H. Hoang *et al.*, Phys. Rev. **D59**, 074017 (1999).
57. H. Leutwyler, Phys. Lett. **B98**, 447 (1981);
    M.B. Voloshin, Sov. J. Nucl. Phys. **36**, 143 (1982).
58. A.H. Hoang, Phys. Rev. **D61**, 034005 (2000).
59. S.E. Csorna *et al.* (CLEO Collab.), Phys. Rev. **D70**, 032002 (2004).
60. A.H. Mahmood *et al.* (CLEO Collab.), Phys. Rev. **D70**, 032003 (2004).
61. B. Aubert *et al.* (BABAR Collab.), Phys. Rev. **D69**, 111103 (2004).
62. B. Aubert *et al.* (BABAR Collab.), Phys. Rev. **D69**, 111104 (2004).
63. C. Schwanda *et al.* (Belle Collab.), Phys. Rev. **D75**, 032005 (2007).
64. P. Urquijo *et al.* (Belle Collab.), Phys. Rev. **D75**, 032001 (2007).
65. J. Abdallah *et al.* (DELPHI Collab.), Eur. Phys. J. **C45**, 35 (2006).
66. D. Acosta *et al.* (CDF Collab.), Phys. Rev. **D71**, 051103 (2005).
67. B. Aubert *et al.* (BABAR Collab.), Phys. Rev. **D81**, 032003 (2010).
68. A. Limosani *et al.* [Belle Collab.], Phys. Rev. Lett. **103**, 241801 (2009).
69. C. Schwanda *et al.* (Belle Collab.), Phys. Rev. **D78**, 032016 (2008).
70. B. Aubert *et al.* (BABAR Collab.), Phys. Rev. **D72**, 052004 (2005).
71. B. Aubert *et al.* (BABAR Collab.), Phys. Rev. Lett. **97**, 171803 (2006).
72. S. Chen *et al.* (CLEO Collab.), Phys. Rev. Lett. **87**, 251807 (2001).
73. M. Battaglia *et al.* Phys. Lett. **B556**, 41 (2003).
74. B. Aubert *et al.* (BABAR Collab.), Phys. Rev. Lett. **93**, 011803 (2004).
75. O. Buchmüller and H. Flächer, `hep-ph/0507253`; updated in Ref. 5.
76. C.W. Bauer *et al.*, Phys. Rev. **D70**, 094017 (2004); updated in Ref. 5.
77. P. Gambino and C. Schwanda, Phys. Rev. **D89**, 014022 (2014).

78. A. Alberti *et al.*, Phys. Rev. Lett. **114**, 061802 (2015).
79. See section 5.4.2 of M. Antonelli *et al.*, Phys. Reports **494**, 197 (2010).
80. B.Dehnadi, *et al.*, JHEP **1309**, 103 (2013).
81. I. Allison *et al.* (HPQCD Collab.), Phys. Rev. **D78**, 054513 (2008).
82. K.G. Chetyrkin *et al.*, Phys. Rev. **D80**, 074010 (2009).
83. T. Ewerth, P. Gambino, and S. Nandi, Nucl. Phys. **B830**, 278 (2010).
84. A.H. Hoang *et al.*, Phys. Rev. **D59**, 074017 (1999).
85. N. Uraltsev, Int. J. Mod. Phys. **A14**, 4641 (1999).
86. M. Neubert, Phys. Rev. **D49**, 4623 (1994); *ibid.* **D49**, 3392 (1994).
87. I. Bigi *et al.*, Int. J. Mod. Phys. **A9**, 2467 (1994).
88. C. W. Bauer *et al.*, Phys. Rev. **D68**, 094001 (2003).
89. M. Neubert, Phys. Lett. **B513**, 88 (2001); Phys. Lett. **B543**, 269 (2002).
90. A.K. Leibovich *et al.*, Phys. Rev. **D61**, 053006 (2000); Phys. Rev. **D62**, 014010 (2000); Phys. Lett. **B486**, 86 (2000); Phys. Lett. **B513**, 83 (2001).
91. A.H. Hoang *et al.*, Phys. Rev. **D71**, 093007 (2005).
92. B. Lange *et al.*, JHEP **0510**, 084 (2005); B. Lange, JHEP **0601**, 104 (2006).
93. M. Neubert, Phys. Lett. **B612**, 13 (2005).
94. Z. Ligeti, I.W. Stewart, and F.J. Tackmann, Phys. Rev. **D78**, 114014 (2008).
95. P. Gambino, K. Healy, and C. Mondino, Phys. Rev. **D94**, 014031 (2016) Phys. Rev. **D78**, 114014 (2008).
96. M. Beneke, F. Campanario, T. Mannel and B. D. Pecjak, JHEP **0506**, 071 (2005).
97. B.O. Lange, M. Neubert, and G. Paz, Phys. Rev. **D72**, 073006 (2005).
98. P. Gambino *et al.*, JHEP **0710**, 058 (2007).
99. J.R. Andersen and E. Gardi, JHEP **0601**, 097 (2006).
100. C.W. Bauer, Z. Ligeti, and M. E. Luke, Phys. Rev. **D64**, 113004 (2001); Phys. Lett. **B479**, 395 (2000).
101. C. Greub, M. Neubert, and B.D. Pecjak, Eur. Phys. J. **C65**, 501 (2010).
102. M. Brucherseifer, F. Caola, and K. Melnikov, Phys. Lett. **B721**, 107 (2013).
103. T. Mannel and S. Recksiegel, Phys. Rev. **D60**, 114040 (1999).
104. I.I.Y. Bigi and N.G. Uraltsev, Nucl. Phys. **B423**, 33 (1994).
105. M.B. Voloshin, Phys. Lett. **B515**, 74 (2001).
106. Z. Ligeti, M. Luke, and A.V. Manohar, Phys. Rev. **D82**, 033003 (2010).
107. P. Gambino and J.F. Kamenik, Nucl. Phys. **B840**, 424 (2010).
108. J. Rosner *et al.* (CLEO Collab.), Phys. Rev. Lett. **96**, 121801 (2006).
109. R. Barate *et al.* (ALEPH Collab.), Eur. Phys. J. **C6**, 555 (1999).
110. M. Acciarri *et al.* (L3 Collab.), Phys. Lett. **B436**, 174 (1998).
111. G. Abbiendi *et al.* (OPAL Collab.), Eur. Phys. J. **C21**, 399 (2001).
112. P. Abreu *et al.* (DELPHI Collab.), Phys. Lett. **B478**, 14 (2000).
113. A. Bornheim *et al.* (CLEO Collab.), Phys. Rev. Lett. **88**, 231803 (2002).
114. A. Limosani *et al.* (Belle Collab.), Phys. Lett. **B621**, 28 (2005).
115. B. Aubert *et al.* (BABAR Collab.), Phys. Rev. **D73**, 012006 (2006).
116. B. Aubert *et al.* (BABAR Collab.), Phys. Rev. Lett. **95**, 111801 (2005), Erratum: Phys. Rev. Lett. **97**, 019903 (2006).
117. R. Kowalewski and S. Menke, Phys. Lett. **B541**, 29 (2002).

118. J.P. Lees *et al.* (BABAR Collab.), Phys. Rev. **D86**, 032004 (2012).
119. I. Bizjak *et al.* (Belle Collab.), Phys. Rev. Lett. **95**, 241801 (2005).
120. P. Urquijo *et al.* (Belle Collab.), Phys. Rev. Lett. **104**, 021801 (2010).
121. J. P. Lees *et al.* (BABAR Collab.), Phys. Rev. **D95**, 072001 (2017).
122. B. Aubert *et al.* (BABAR Collab.), Phys. Rev. Lett. **96**, 221801 (2006).
123. H. Kakuno *et al.* (Belle Collab.), Phys. Rev. Lett. **92**, 101801 (2004).
124. A. Sibidanov *et al.* (Belle Collab.), Phys. Rev. **D88**, 032005 (2013).
125. B. Aubert *et al.* (BABAR Collab.), Phys. Rev. Lett. **90**, 181801 (2003).
126. T. Hokuue *et al.* (Belle Collab.), Phys. Lett. **B648**, 139 (2007).
127. B. Aubert *et al.* (BABAR Collab.), Phys. Rev. **D79**, 052011 (2008);
J. P. Lees *et al.* (BaBar Collab.), Phys. Rev. **D88**, 072006 (2013);
J. P. Lees *et al.* (BaBar Collab.), Phys. Rev. **D87**, 032004 (2013).
128. C. Schwanda *et al.* (Belle Collab.), Phys. Rev. Lett. **93**, 131803 (2004).
129. N. E. Adam *et al.* (CLEO Collab.), Phys. Rev. Lett. **99**, 041802 (2007);
Phys. Rev. **D76**, 012007 (2007); supercedes Phys. Rev. **D68**, 072003 (2003).
130. P. del Amo Sanchez *et al.*, (BABAR Collab.), Phys. Rev. **D83**, 032007 (2011);
supercedes B. Aubert *et al.* (BABAR Collab.), Phys. Rev. **D72**, 051102 (2005).
131. P. del Amo Sanchez *et al.*, (BABAR Collab.), Phys. Rev. **D83**, 052011 (2011);
updated in J.P. Lees *et al.* (BABAR Collab.), Phys. Rev. **D86**, 092004 (2012).
132. J.A. Bailey *et al.* (Fermilab/MILC Collab.), Phys. Rev. **D92**, 014024 (2015).
133. C.M. Bouchard *et al.*, Phys. Rev. **D90**, 054506 (2014).
134. J.M. Flynn *et al.*, Phys. Rev. **D91**, 074510 (2015).
135. T. Becher and R. J. Hill, Phys. Lett. **B633**, 61 (2006).
136. M.C. Arnesen *et al.*, Phys. Rev. Lett. **95**, 071802 (2005).
137. M.A. Shifman, A.I. Vainshtein, and V.I. Zakharov, Nucl. Phys. **B147**, 385 (1979);
Nucl. Phys. **B147**, 448 (1979).
138. P. Ball and R. Zwicky, Phys. Rev. **D71**, 014015 (2005).
139. G. Duplancic *et al.*, JHEP **0804**, 014 (2008).
140. A. Khodjamirian *et al.*, Phys. Rev. **D83**, 094031 (2011).
141. A. Bharucha, JHEP **1205**, 092 (2012).
142. I.S. Imsong *et al.*, JHEP **1502**, 126 (2015).
143. H. Ha *et al.* (Belle Collab.), Phys. Rev. **D83**, 071101 (2011).
144. K. Abe *et al.* (Belle Collab.), Phys. Lett. **B648**, 139 (2007).
145. B. Aubert *et al.* (BABAR Collab.), Phys. Rev. Lett. **101**, 081801 (2008).
146. B. Aubert *et al.* (BABAR Collab.), Phys. Rev. Lett. **97**, 211801 (2006).
147. Y. Amhis *et al.* (HFAG), `arXiv:1412.7515`.
148. W. Brower and H. Paar, Nucl. Instrum. Methods **A421**, 411 (1999).
149. C. Bourrely, I. Caprini, and L. Lellouch, Phys. Rev. **D79**, 013008 (2009).
150. P. Ball, `arXiv:0705.2290`;
J.M. Flynn and J. Nieves, Phys. Lett. **B649**, 269 (2007);
T. Becher and R.J. Hill, Phys. Lett. **B633**, 61 (2006);
M. Arnesen *et al.*, Phys. Rev. Lett. **95**, 071802 (2005).
151. S. Aoki *et al.*, (FLAG working group), Eur. Phys. J. **C77**, 112 (2017).
152. A. Barucha, JHEP **05**, 092 (2012).

153. T. Feldmann and M.W.Y. Yip, Phys. Rev. Lett. **85**, 014035 (2012).
154. W. Detmold, C. Lehner, and S. Meinel, Phys. Rev. **D92**, 034503 (2015).
155. The LHCb Collab., Nature Physics **11**, 743 (2015).
156. M. Ablikim *et al.*, (BESIII Collab.), Phys. Rev. Lett. **116**, 052001 (2016).
157. The LHCb Collab., arXiv:1709.01920.
158. M. Tanaka, Z. Phys. **C67**, 321 (1995);
H. Itoh, S. Komine, and Y. Okada, Prog. Theor. Phys. **114**, 179 (2005);
U. Nierste, S. Trine, and S. Westhoff, Phys. Rev. **D78**, 015006 (2008);
M. Tanaka and R. Watanabe, Phys. Rev. **D82**, 034027 (2010).
159. H. Na *et al.*, Phys. Rev. **D92**, 054510 (2015). Erratum ibid. **D93**, 119906 (2016).
160. J.F. Kamenik and F. Mescia, Phys. Rev. **D78**, 014003 (2008).
161. S. Fajfer, J. F. Kamenik, and I. Nišandžić, Phys. Rev. **D85**, 094025 (2012).
162. S. Aoki *et al.* (FLAG working group), Eur. Phys. J. **C77**, 112 (2017).
163. D. Bigi and P. Gambino, Phys. Rev. **D94**, 094008 (2016).
164. B. Aubert *et al.* (Babar Collab.), Phys. Rev. Lett. **100**, 021801 (2008).
165. J. Lees *et al.* (Babar Collab.), Phys. Rev. Lett. **109**, 101802 (2012); Phys. Rev. **D88**, 072012 (2013).
166. M. Huschle *et al.* (Belle Collab.), Phys. Rev. **D92**, 072014 (2015).
167. Y. Sato *et al.* (Belle Collab.), Phys. Rev. **D94**, 072007 (2016).
168. S. Hirose *et al.* (Belle Collab.), Phys. Rev. Lett. **118**, 211801 (2017).
169. The LHCb Collab., Phys. Rev. Lett. **115**, 111803 (2015).
170. The LHCb Collab., arXiv:1708.08856.
171. http://www.slac.stanford.edu/xorg/hfag/semi/fpcp17/RDRDs.html.
172. A. Datta, M. Duraisamy, and D. Ghosh, Phys. Rev. **D86**, 034027 (2012).
173. D. Becirevic, N. Kosnik, and A. Tayduganov, Phys. Lett. **B716**, 208 (2012).
174. S. Fajfer *et al.*, Phys. Rev. Lett. **109**, 161801 (2012).
175. A. Crivellin, C. Greub, and A. Kokulu, Phys. Rev. **D86**, 054014 (2012).
176. M. Bauer and M. Neubert, Phys. Rev. Lett. **116**, 141802 (2016).
177. I. Doršner et al., Phys. Rept. **641**, 1 (2016).
178. A. Celis et al., Phys. Lett. **B771**, 168 (2017).
179. J. G. Körner and G. A. Schuler, Z. Phys. **C46**, 93 (1990).
180. M. Tanaka and R. Watanabe, Phys. Rev. **D87**, 034028 (2013).
181. A. Matyja *et al.* (Belle Collab.), Phys. Rev. Lett. **99**, 191807 (2007).
182. A. Bozek *et al.* (Belle Collab.), Phys. Rev. **D82**, 072005 (2010).
183. P. Hamer *et al.* (Belle Collab.), arXiv:1509.06521.
184. USQCD Collab. (2011),
www.usqcd.org/documents/HiIntensityFlavor.pdf.